https://doi.org/10.15407/ufm.27.03.494

V.B. TARELNYK [1,*], O.P. HAPONOVA [2,3,], Ie.V. KONOPLIANCHENKO [1,***], N.V. TARELNYK [1,****], S.G. BONDAREV [1,*****], and M.O. MIKULINA [1,******]**

[1] Sumy National Agrarian University,
160 Herasyma Kondratieva St., 40021 Sumy, Ukraine
[2] Sumy State University,
116 Kharkivska St., 40007 Sumy, Ukraine
[3] Institute of Fundamental Technological Research,
Polish Academy of Sciences,
5B Pawińskiego, 02-016 Warsaw, Poland

* tarelnyk@ukr.net, ** gaponova@pmtkm.sumdu.edu.ua,
*** konoplyanchenko@ukr.net, **** natashatarelnik@ukr.net,
***** mr-bond@i.ua, ****** marinamikulina1@ukr.net

IMPROVING THE QUALITY PARAMETERS OF STEEL SURFACES BY COMBINED ELECTROSPARK CARBURIZING TECHNOLOGIES. Pt. 2. Mathematical Models for Controlling the Properties of Metal Surfaces

Modern mechanical engineering is grounded in the latest advances in science and technology, necessitating the implementation of reliable and fail-safe engineering solutions, which ensure the reliability and durability of machine components operating under severe conditions, including intensive loading, extreme temperatures, and corrosive environments. Addressing these challenges requires the development of technological foundations for surface modification of machine parts, using environmentally benign methods, which remains a pressing and relevant task. The present study demonstrates that, among contemporary technologies, electrospark alloying (ESA) is of particular interest, as it enables the formation of surface-layer structures with unique physicomechanical and tribological properties. The objective of this work is to develop

Citation: V.B. Tarelnyk, O.P. Haponova, Ie.V. Konoplianchenko, N.V. Tarelnyk, S.G. Bondarev, and M.O. Mikulina, Improving the Quality Parameters of Steel Surfaces by Combined Electrospark Carburizing Technologies. Pt. 2. Mathematical Models for Controlling the Properties of Metal Surfaces, *Progress in Physics of Metals*, **27**, No. 3: 496–543 (2026)

an adequate, physically substantiated mathematical model for predicting the quality parameters of surface layers of steel components during electrospark carburizing (ESC) and electrospark nitrocarburizing (ESNC) as functions of the energy and technological parameters of ESA equipment, employing a specialised saturating technological medium (SSTM). The paper presents the results of investigations of the influence of preliminary aluminium treatment on the quality parameters of modified steel surfaces, using an SSTM composed of nitrogen–carbon constituents. Phase-composition analysis reveals that the presence of an aluminium interlayer leads to the formation of aluminium-containing phases, resulting in a significant increase in both hardness and thickness of the surface layers. Experimental dependences of surface quality parameters on the energy and technological parameters of ESA during ESNC and ESC processes are established. Based on the conducted research, mathematical models describing the dependence of surface quality on ESNC and ESC are developed, including equations for the increment of the hardened-layer thickness and the increment of surface microhardness as functions of ESA-equipment parameters. These models enable the determination of key technological characteristics of the formed layer, namely, the thickness of the hardened layer and its microhardness. A methodology for determining the constants of the increment equations for ESNC and ESC processes is developed. This includes the evaluation of both hardened-layer thickness (considering the maximum increment as a function of discharge energy, process-intensiveness, and activation energy) and microhardness (considering the maximum increment as a function of discharge energy, process-intensiveness, and activation energy). The proposed mathematical models can be applied for strengthening the surface layers of components in compressor and pumping equipment, including protective sleeves, end faces of rings, mating surfaces of casings and covers, and bearing journals of centrifugal machinery shafts, *etc*.

Keywords: electrospark alloying, carburizing, nitrocarburizing, hardened layer, mathematical modelling.

1. Introduction

Work [1] presents the urgency of the research, which is conditioned by the growing requirements for the reliability and durability of the machine parts operating under intense mechanical loads [2, 3], elevated temperatures and the action of corrosive environments [4–6].

An analysis of the modern technologies for improving the quality of the surface layers of the parts has been carried out, namely, chemical–thermal treatment (CTT) [7–9], gas–thermal spraying the metal–ceramic coatings [10], welding the coatings formed by composite materials [11], performing the centrifugal reinforcement with tungsten carbide [12], applying the aluminium-oxide layer coatings [13–15], as well as using the plasma and detonation spraying methods [16–19], *etc*. In addition, there are technologies aimed at improving the surface operational properties even at design stages [20–24], along with a series of theoretical models [25–30] contributing to the analysis of structural changes and to improving the prediction of bulk- and surface-related parameters of aluminium-containing alloys subjected to external treatments (particularly, surface treatments such as electrospark alloying (ESA)).

In addition, in Ref. [1], the technology for increasing the wear resistance of the surfaces due to the multilayer coatings of hard wear-resistant and soft antifriction materials [31–34], and the technology using modern composite materials, which have increased wear resistance of surfaces, high strength and toughness [35–37] have been considered. There has been carried out an analysis of energy-efficient technologies for processing materials with the use of concentrated energy flows (CEF), namely, by ion nitriding [38, 39], condensed ion bombarding [39–41], plasma spraying [42–45] and plasma processing [46, 47], as well as laser processing [48–51]. It has been emphasized that, among the technologies implemented with the CEF, the most noteworthy technologies are the ones which use the ESA method.

Owing to the ESA methods, structures with unique physicomechanical and tribological properties at the nanolevel are formed in the surface layers [52–54]. In Refs. [55–57], the advantages of the ESA method over the traditional technologies for surface treatment of parts have been considered. In Refs. [58–62], there have been analyzed the ESA technology disadvantages, which, when in combination with the other methods for strengthening the surfaces of the parts, such as the ESA + the application of the metal-polymer materials (MPM), act as advantages.

Depending on the ESA method, alloying medium, cathode and anode materials, the properties of the surface layers are sufficiently presented in Refs. [33, 63–67].

With the use of a special technological saturating medium (STSM), the ESA method, namely, aluminizing [68], carburizing [69–71], and nitriding [72], can be used to obtain not only single-component coatings, but also multicomponent ones [73, 74].

In Refs. [75, 76], the wide possibilities of using graphite as an anode during the ESA process have been proven. The free-state graphite is an effective solid lubricant, and in the bound state, particularly in the form of carbides, it acts as a solid wear-resistant phase. During the ESA process, the surface of the part is saturated with carbon by a graphite electrode, which gives grounds to compare it with a type of the CTT process, namely, carburizing [77–79].

Considering that with the traditional CTT, during nitriding, the best results, in terms of hardness and depth of the strengthened layer, are achieved, when processing alloyed and high-value steels containing aluminium, the use of the STSMs allows for conducting the ESA process with aluminium for the cheaper steels, such as 40, 45, 50, 40X (40Kh), *etc.*, and after that, nitriding the surface layers thereof [80].

Thus, the analysis of the ESA technologies with a graphite electrode-tool (ET) has shown that, despite the wide range of applications, unfortunately, there is no correlation relationship between the quality parameters of steel surfaces after the process of electrospark carburizing (ESC) and nitrocarburizing by the ESA method (NESC) and the energy and technological parameters of the ESA equipment. The importance of conducting further research is determined by the formulation of the purpose of the work.

The purpose of the work is to develop an adequate and physically based mathematical model for predicting the quality parameters of the steel part surface layers during the ESC and NESC processes, depending on the energy and technological parameters of the ESA equipment when using the STSMs.

To achieve this goal, the following technical problems must be solved:

- to investigate the quality parameters of the surfaces of steel parts formed by the ESC method in the presence of an aluminium sublayer, using the saturating media containing N + C components;
- to determine and analyse the dependence of the quality parameters of the part surfaces on the energy and technological parameters of the ESA using the STSMs during the processes of nitrocarburizing and carburizing;
- to develop a mathematical model for predicting the quality parameters of the surface layers of steel parts during the NESC process using the ESA method;
- to develop a mathematical model for predicting the quality parameters of the surface layers of steel parts during the ESC process using the ESA method.

In Ref. [81], a new, environmentally friendly and effective process for nitriding steel surfaces has been developed to ensure high durability of steel parts. The process included the following stages: applying the STSM, which is used as a pasty nitrogen component, to the working surface and, without waiting for it to dry, carrying out the treatment of the ESA by the ET made of a material identical to the material of the steel part being processed.

When using this process for nitriding C22 steel and C40 steel, with an increase in discharge energy from 0.13 to 3.4 J, the following parameters increase: the thickness of the 'white' layer from 10 to 40 μm and from 10 to 50 μm, respectively, its microhardness from 6228 to 8969 MPa and from 6860 to 9160 MPa, respectively, the surface roughness (R_a) from 0.9 to 6.2 μm and from 0.9 to 5.9 μm, respectively, and the continuity of the coating from 50% to 70% and from 60% to 80%, respectively.

The wear resistance of the nitrided surfaces increases as compared to the untreated samples by 219% and 308% for steel 20 and steel 40, respectively.

The disadvantages of this process are the small thickness of the 'white' layer and its relatively low microhardness.

It is known from Ref. [82] that, to obtain high-hardness steel in the nitriding process, the aluminium-containing and improved steels $41CrAlMo_7$, $42CrMo_4$ and $34CrAl_6$ are used as the bases. This has been confirmed in

Ref. [83], according to which nitrided steel is characterised by its high durability, wear resistance, corrosion resistance, hardness and other favourable properties.

Taking into account the advantages and disadvantages of the above processes, a new process implementing the ESA method has been proposed. When using this process, before applying the STSM to the surface being strengthened, an Al layer has been applied thereto by the ESA method at discharge energy $W_p = 0.13–6.8$ J.

A promising direction for increasing the resource of machine parts is the CTT process, namely, the nitrocarburizing process, which makes it possible to increase both the mechanical properties (strength, hardness, fatigue limit) and the corrosion resistance. The nitrocarburized layer provides the parts with sufficient toughness and high strength. The nitrocarburized coatings have high resistance to abrasion, which is associated with the formation of the N-containing phases [84].

The high-speed nitrocarburized process has certain advantages. These include the short processing time, no need for special surface preparation, and the availability of accurate localisation of the method [85].

According to Ref. [86], the authors have developed a method for strengthening the surfaces of the heat-treated steel parts. The method includes ESC processing and differs in that nitrogen is supplied into the alloying zone. In this case, two processes are being carried out simultaneously, namely the ESC process and the nitriding one. These are actually operating as a NESC process.

It should be noted that the implementation of this process requires the constant presence of nitrogen, and rather high consumption thereof significantly reduces its advantages.

According to Refs. [87, 88], a new environmentally safe and effective nitrocarburizing process has been proposed. It is carried out by the ESA method, including the stage of applying a pasty carburizer containing nitrogen–carbon components to the surface being strengthened. This pasty carburizer, without waiting for it to dry, is processed with a graphite ET.

During NESC processing the samples made of C22 steel and C40 steel, with an increase in the discharge energy from 0.13 to 3.4 J, the following parameters there increase: the thickness of the ‘white’ layer from 10 μm to 110 μm and from 20 μm to 120 μm, respectively; its microhardness from 6.665 to 9.731 and from 7.135 to 9.932 MPa, respectively; the surface roughness (R_a) from 0.8 to 4.1 μm and from 0.9 to 4.7 μm, respectively; the coating continuity from 80 to 100% and from 90 to 100%, respectively.

While processing at all the discharge energies being studied, the largest amounts of carbon and nitrogen have been located closer to the surface, and they have been decreasing with increasing depths of their locations. Increasing the ESA discharge energy from 0.13 to 3.4 J leads to an increase in the parameters of the carbon and nitrogen diffusion zones, namely, for carbon, from 20 to 45, and for nitrogen, from 20 to 55 μm.

The disadvantages of this process are the small thickness of the 'white' layer and its relatively low microhardness.

According to Ref. [89], a new environmentally safe and effective carburizing process has been proposed. It is carried out by the ESA method, and includes the stage of applying a pasty carburizer containing 80% graphite powder and 20% petroleum jelly to the surface being strengthened while this pasty carburizer, without waiting for it to dry, is being processed by a graphite ET.

It should be noted that due to the analysis of the above-mentioned works aimed at improving the quality of the surface layers of the steel parts, it has been found that from the point of view of efficiency, environmental safety, cost, *etc.*, the technologies based on the ESA method are considered the most promising.

At the same time, owing to the use of the stage of applying a paste-like carburizer containing nitrogen–carbon components to the strengthened surface, and because these components exhibit their maximum activities at different temperatures (500–900 °C), it is possible to process the steel products, while using various methods for processing, namely: from practically purely nitriding to nitrocarburizing and carburizing. In addition, ESA processing of aluminium-strengthened carbon steel surfaces can improve the quality parameters of the surface layers.

2. Materials and Methods

Before applying the STSM to the surface being strengthened, an aluminium layer is applied by the ESA method with W_p = 0.13–6.80 J.

The samples were made of C22 and C40 steels and had a size of 15×15×8 mm.

To perform the aluminium deposition, a unit of 'Elitron-52A' model was used, providing a discharge energy W_p in the range of 0.05 to 6.80 J. For the study, the values of W_p = 0.13, 0.52, and 3.40 J were used. Aluminium had been deposited by the ET in the form of an aluminium wire having a diameter of 3.0 mm, AD grade, according to GOST 14838-78. For ESA processing with a material identical to the material of the part being processed, the modes of W_p = 0.13, 0.52, and 3.40 J were used. At the nitriding process, a pasty mixture prepared by mixing 10% petroleum jelly with urea powder (≈90%) was used as the STSM; at the nitrocarburizing process, the paste-like mixture was prepared with the use of urea (45%), yellow blood salt (45%) and petroleum jelly (10%), and at ESC processing, the paste-like mixture was prepared with the use of graphite powder (80%) and petroleum jelly (20%).

The metallographic and durometric studies were carried out according to the known technologies and with the use of the appropriate equipment.

At all stages of processing, the surface roughness was measured using a profilograph-profilometer of model 201 manufactured by the 'Calibre' plant.

The STSM in the form of a paste was applied to the surfaces of the samples after processing the surfaces by the ESA method with the use of an aluminium ET. Then, without waiting for the aforementioned surface to dry, it was processed using the ESA method by the ET in the form of a wire having a diameter of 3 mm, made of a material identical to the material of the steel part being processed, while nitriding, or by the electrode-tool (ET) in the form of a graphite rod of the EG-4 brand measuring 3×3×25 mm, while nitrocarburizing and in the course of the ESC process.

X-ray structural analysis was performed on the DRON-3 diffractometer in CoK_α-radiation. The voltage and anode current were 30 kV and 24 mA, respectively. The x-ray diffractograms were taken by step-by-step scanning with an exposure of 2 s at each point. The experimental results were processed using special software.

3. Results and Discussions

Figure 1 shows the microstructure after the ESA process with the use of an aluminium ET at $W_p = 3.4$ J. Due to the analysis of Fig. 1, it has been found that the coating consists of three zones, namely: the 'white' layer, the diffusion zone and the base metal.

It should be noted that the coating parameters depend on the discharge energy and W_p during the ESA process. With increasing W_p, the continuity of the 'white' layer, its thickness and microhardness increase. The surface roughness also increases.

Figure 2 shows the microstructure of the surface layer of a C40 steel sample after the nitrocarburizing process by the ESA method, which includes the following stages: obtaining an aluminium sublayer by the ESA method with the use of an aluminium ET at $W_p = 3.40$ J; applying a nitrogen-containing paste to the surface being processed; further alloying the surface being processed with a graphite ET at $W_p = 0.13$,

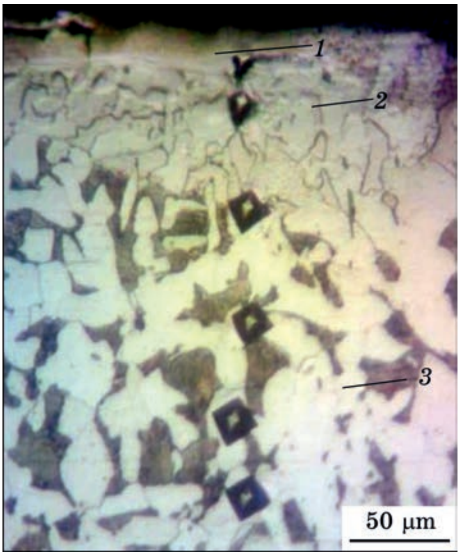

Fig. 1. Microstructure of the surface layer of a C22 steel sample after the ESA using the aluminium ET: *1* — 'white' layer, *2* — diffusion zone, *3* — substrate [80]

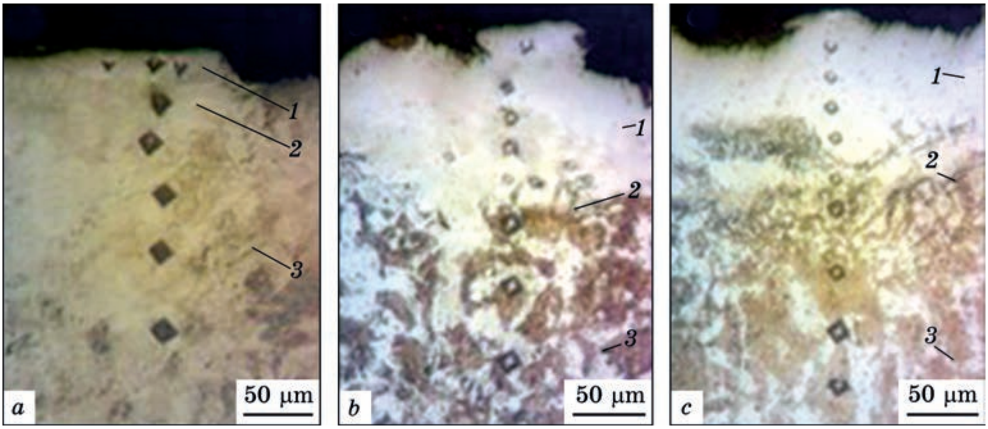

Fig. 2. Microstructures of nitrocarburized surface layers of the C40 steel samples with Al sublayers and processed *via* the ESA by the ET formed of C40 steel at: (*a*) — W_p = 0.13, (*b*) — W_p = 0.52, and (*c*) — W_p = 3.40 J, where *1* — 'white' layer, *2* — diffusion zone, and *3* — substrate [80]

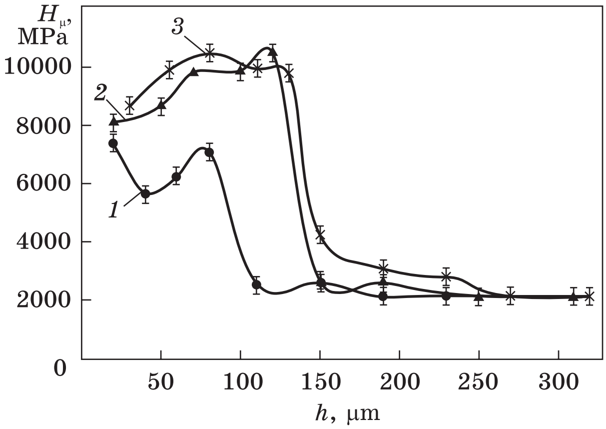

Fig. 3. Microhardness distribution along the surface depth of a C40 steel sample after the ESA using aluminium ET at W_p = 3.4 J, applying nitrogen-containing paste to the processed surface, and alloying the resulting surface with a graphite ET at W_p = 0.13 (*1*), 0.52 (*2*), 3.40 (*3*) J [80]

0.52, and 3.40 J, respectively. As compared to the nitriding process, after the nitrocarburizing process, the thickness of the 'white' layer and the diffusion zone is greater. This is apparently because nitrocarburizing is carried out with the use of a graphite ET, unlike nitriding, where an ET made of steel is used. The microstructure shows a visible section having incomplete recrystallization. For C40 steel, this is heating to a temperature of 730–755 °C. The metal in this section undergoes incomplete recrystallization. The base metal (C40 steel) has a ferrite–pearlite structure.

Figure 3 shows a graph of the distribution of microhardness in the surface layer after the nitrocarburizing process by the ESA method. In the graph: *1*, *2*, and *3* — with the aluminium sublayer obtained by the ESA method using the aluminium ET at W_p = 3.40 J, as well as by the ESA method using a graphite ET at W_p = 0.13, 0.52, and 3.4 J, respectively.

The results of measuring the thickness, microhardness and continuity of the 'white' layer, as well as the surface roughness of the C22 steel sample and the C40 steel sample, each after the nitrocarburizing process, are given in Table 1. After the nitrocarburizing process, the thickness parameter of the deposited layer increases more intensively with the higher value of the discharge energy at which the aluminium sublayer is deposited. The microhardness and continuity of the 'white' layer had been increasing while previously ESA processing by aluminium, but in that case, the roughness changed insignificantly.

Table 1. **The qualitative parameters of the nitrocarburized (N + C) layers obtained by the ESA method on C22 steel and C40 steel [80]**

Discharge energy, J	Thickness of the 'white' layer, μm	Microhardness of the 'white' layer, MPa	Roughness, μm			Continuity of the 'white' layer, %
			R_a	R_z	R_{max}	
Without aluminium sublayer						
C22 Steel						
0.13	10–20	6665	0.9	1.9	6.5	80
0.52	30–40	7689	1.2	2.1	8.1	90
3.40	80–110	9731	4.1	11.3	25.1	100
C40 Steel						
0.13	20–30	7135	0.9	2.2	7.3	80
0.52	30–50	7920	1.3	2.7	8.7	90
3.40	80–120	9930	4.7	16.2	35.1	100
With aluminium sublayer at W_p = 0.13 J						
C22 Steel						
0.13	10–25	6850	0.9	1.9	7.5	80
0.52	10–30	8010	1.5	2.1	8.3	90
3.40	30–40	9930	5.6	12.4	28.5	100
With aluminium sublayer at W_p = 0.52 J						
C22 Steel						
0.13	20–35	6900	0,9	2.0	7.5	85
0.52	30–45	8300	1.7	2.2	8.7	100
3.40	50–70	9800	5.7	12.7	28.7	100
With aluminium sublayer at W_p = 3.4 J						
C22 Steel						
0.13	60–70	7150	1.1	2.1	7.5	90
0.52	60–80	9721	1.6	2.3	9.1	100
3.40	90–110	10050	5.9	13.3	28.9	100
With aluminium sublayer at W_p = 0.13 J						
C40 Steel						
0.13	50–70	7320	1.2	2.2	7.3	100
0.52	60–80	10380	1.9	2.9	8.7	100
3.40	80–110	10380	6.3	16.8	31.1	100

Table 2 summarizes the results of measuring the thickness, microhardness and continuity values of the 'white' layer, as well as the surface roughness of the C22 steel sample after the ESC process, which consisted of the procedures of alloying the surface by the ESA method with the use of an aluminium ET at W_p = 0.13, 0.52, and 3.40 J, applying a carbon-containing paste to the surface being processed, and treating the resulting surface by the ESC at W_p = 0.13, 0.52 and 3.4 J. The thickness and microhardness of the 'white' layer had been increasing, while the previous ESA by aluminium and the continuity had not been changing there. After the ESC process, the thickness of the strengthened layer had been increasing

Table 2. **The qualitative parameters obtained by the ESC process for C22 steel and C40 steel [80]**

Discharge energy, J	Thickness of the 'white' layer, μm	Microhardness of the 'white' layer, MPa	Roughness, R_a, μm	Continuity of the 'white' layer, %
		Without aluminium sublayer		
		C22 Steel		
0.9	50–70	9932	1.0	100
2.6	80–100	10796	3.7	
4.6	100–230	10796	4.8	
		C40 Steel		
0.9	60–80	11351	1.0	100
2.6	90–110	11787	3.8	
4.6	130–240	11824	4.7	
		With aluminium sublayer at W_p = 0.13 J		
		C22 Steel		
0.9	55–75	10153	1.0	100
2.6	85–110	11930	3.6	
4.6	100–230	11995	4.8	
		With aluminium sublayer at W_p = 0.52 J		
		C22 Steel		
0.9	60–80	10320	1.0	100
2.6	90–120	11950	3.8	
4.6	130–240	12100	4.8	
		With aluminium sublayer at W_p = 3.4 J		
		C22 Steel		
0.9	70–90	10370	1.0	100
2.6	100–130	12050	3.7	
4.6	140–260	12200	4.9	
		With aluminium sublayer at W_p = 0.13 J		
		C40 Steel		
0.9	80–100	11760	1.0	100
2.6	110–140	12240	3.7	
4.6	140–280	12375	4.9	

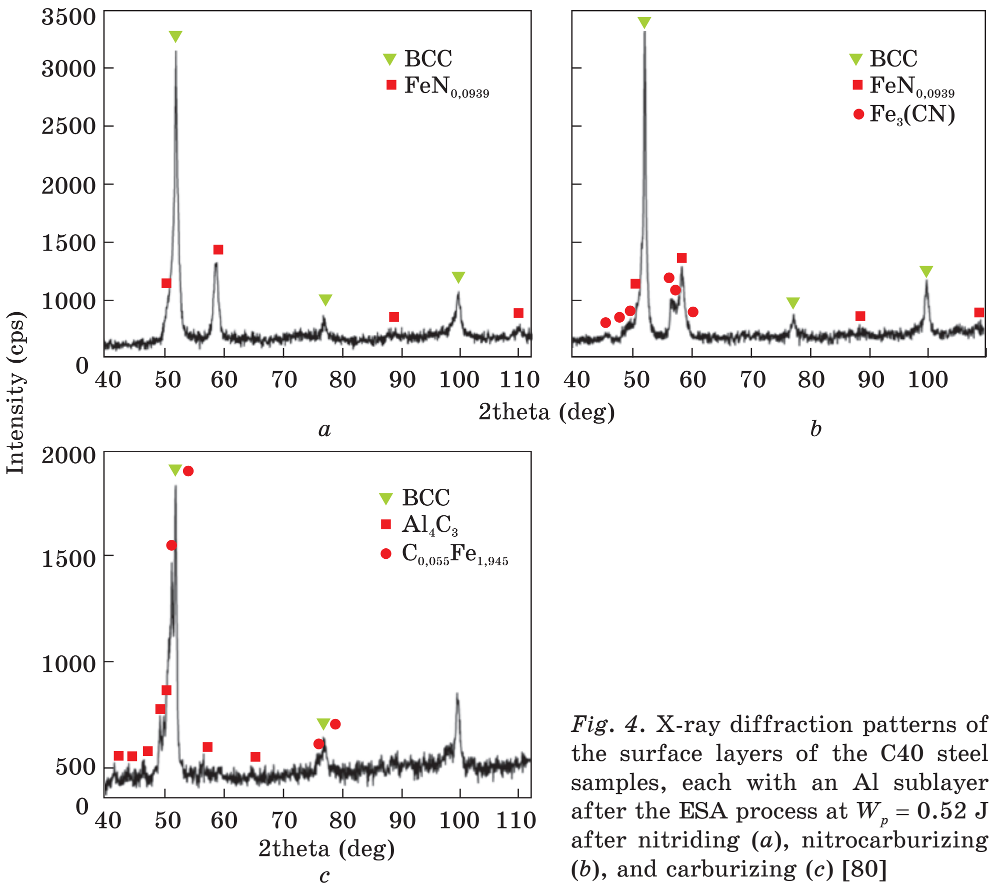

Fig. 4. X-ray diffraction patterns of the surface layers of the C40 steel samples, each with an Al sublayer after the ESA process at $W_p = 0.52$ J after nitriding (*a*), nitrocarburizing (*b*), and carburizing (*c*) [80]

with increasing discharge energy at which the aluminium sublayer had been applied.

The studies of the phase composition of the obtained coatings on C40 steel have shown that while nitriding, the phase composition has been represented by the b.c.c. solid solution and cubic iron nitride in Fig. 4, *a*. Most likely, aluminium has been dissolving in ferrite and nitride. In addition, there is a possibility of the formation of a sublayer of aluminium-containing phases between the substrate and the nitrogen-containing coating. This is evidenced by the results of the microhardness measurements. During ESA processing, the microhardness of the coating at a distance of ≈70 μm from the surface has been increasing as compared to the values thereof on the surface.

After nitrocarburizing by the ESA method, the presence of a b.c.c. solid solution, cubic iron nitride, and iron carbide has been detected in Fig. 4, *b*. As clearly seen in the figure, in the presented phases, carbon atoms can be partially replaced by nitrogen atoms. In addition, it is quite probable that aluminium dissolves in ferrite and iron nitride, and it is located in the sublayer between the coating and the substrate.

On carburizing the samples with aluminium sublayers obtained after the ESA process, the x-ray diffraction analysis revealed the presence of a b.c.c. solid solution, the diffraction maxima of which were completely overlapped by tetragonal iron carbide $C_{0.055}Fe_{1.945}$. The remaining diffraction maxima are associated with rhombohedral aluminium carbide Al_4C_3.

Analysis of the phase composition of the coatings indicates that the presence of an aluminium sublayer ensures the formation of the phases, the presence of which leads to a significant increase in hardness and contributes to an increase in the thickness and quality values of the surface layers.

Thus, based on the analysis of the studies conducted by the authors of Ref. [80], the conclusions can be formulated as follow.

For C22 and C40 steels, when using nitriding, NESC and ESC processes, with increasing discharge energy, the values of thickness, microhardness and continuity of the 'white' layer, as well as the surface roughness value, increase.

While nitriding, NESC and ESC processing the C22 and C40 steels, previously processed by the ESA method with the use of an aluminium ET, the thickness, microhardness and continuity of the 'white' layer increase, while the roughness changes slightly.

Previously processing by the ESA method using an aluminium ET at $W_p < 0.13$ J does not lead to noticeable changes in the quality parameters of the surface layer formed for all processing types, and at $W_p > 3.40$ J, it is accompanied by a sharp increase in the roughness of the surface layer. For practical application, the recommended discharge energy parameters are in the range of $W_p = 0.13–3.40$ J for nitriding and the NESC process, and those are in the range of $W_p = 0.13–4.60$ J for the ESC process.

The analysis of the phase composition has shown that the presence of the aluminium sublayer leads to the formation of the aluminium-containing phases, which in turn causes a significant increase in the hardness and thickness values of the surface layers.

The proposed methods, *viz.*, nitriding, NESC and ESC, can be used to strengthen the surface layers of critical parts and their elements for compressor and pump equipment: external and internal surfaces of protective sleeves of floating seals, end surfaces of their rings and connecting parts of housings and covers; bearing journals of rotor shafts of centrifugal machines; piston rods, *etc*.

3.1. Determining and Analysing the Quality Parameters of the Part Surfaces Dependent on the Energy and Technological ESA Parameters: STSMs at NESC Processing

The new technologies for performing the synthesis of coatings by the ESA method with the use of the STSMs are considered in Fig. 5.

At all stages of the research, see also Refs. [90, 92, 93], the surface roughness was determined using a profilograph-profilometer device of mod. 201 of the 'Calibre' plant production. To conduct the durometric studies, analyse the Vickers-hardness distribution in the surface layer, and along the depth of the section from the surface, the hardness testers of the PMT-3 and NOVA 330/360 (manufacturer INNOVATEST Europe BV, the Netherlands) models were used in accordance with GOST 2999-75 and ISO 6507. The investigations of the microstructural parameters of the coatings were carried out on the microsections, using such microscopes as the Hirox KH-8700 and MIM-7 optical microscopes, the SEO-SEM Inspect S50-B scanning electron microscope equipped with an energy-dispersive spectrometer of the AZtecOne type with an X-MaxN20 detector (manufactured by Oxford Instruments plc).

Producing the samples, preparing the surfaces and studying the structural parameters were carried out according to Ref. [91].

The values of the ESA productivity were taken in accordance with the recommendations of the ESA equipment manufacturers. Table 3 shows the average data of these recommendations.

Considering that the presence of the STSM in a viscous-liquid state in the ESA zone affects the mass transfer process, to study the influence of

Table 3. **The discharge energy and the productivity recommended for implementation by the ESA equipment suppliers [90]**

Discharge energy W_p, J	0.130	0.52	1.30	2.60	4.60	6.80
Productivity Q, cm^2/min	0.5	1.1	1.4	1.7	2.3	2.8

Table 4. **The dependence of the ESA productivity and labour-intensiveness on W_p values [90]**

Discharge energy W_p, J		0.13	0.52	3.4
Productivity Q, cm^2/min	Option 1	≈0.3	≈0.6	≈1.0
	Option 2	≈0.2	≈0.3	≈0.5
	Option 3	≈0.1	≈0.2	≈0.3
Labour-intensiveness τ, min/cm^2	Option 1	≈3.3	≈1.7	≈1.0
	Option 2	≈5.0	≈3.3	≈2.0
	Option 3	≈10.0	≈5.0	≈3.3

the discharge energy and processing time (labour-intensiveness τ) in the further experiments, the processing time was increased by 2, 3 and 4 times as compared to the recommended values given in Table 3 (Table 4).

According to Ref. [80], pre-alloying with aluminium increases the thickness, microhardness and continuity values of the coating during nitriding, NESC and ESC processing by the ESA method. The best results were achieved when using the ET made of aluminium at a discharge energy $W_p = 3.40$ J; therefore, further studies were carried out using this particular processing technology.

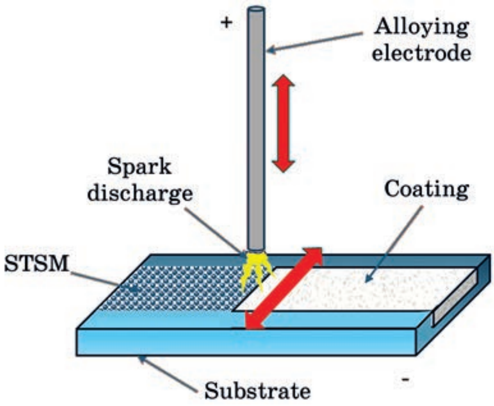

Fig. 5. Scheme of the ESA process [93]

For the STSM, the paste-like mixture of urea and yellow blood salt was used to perform the NESC process; the mixture of 80% graphite powder

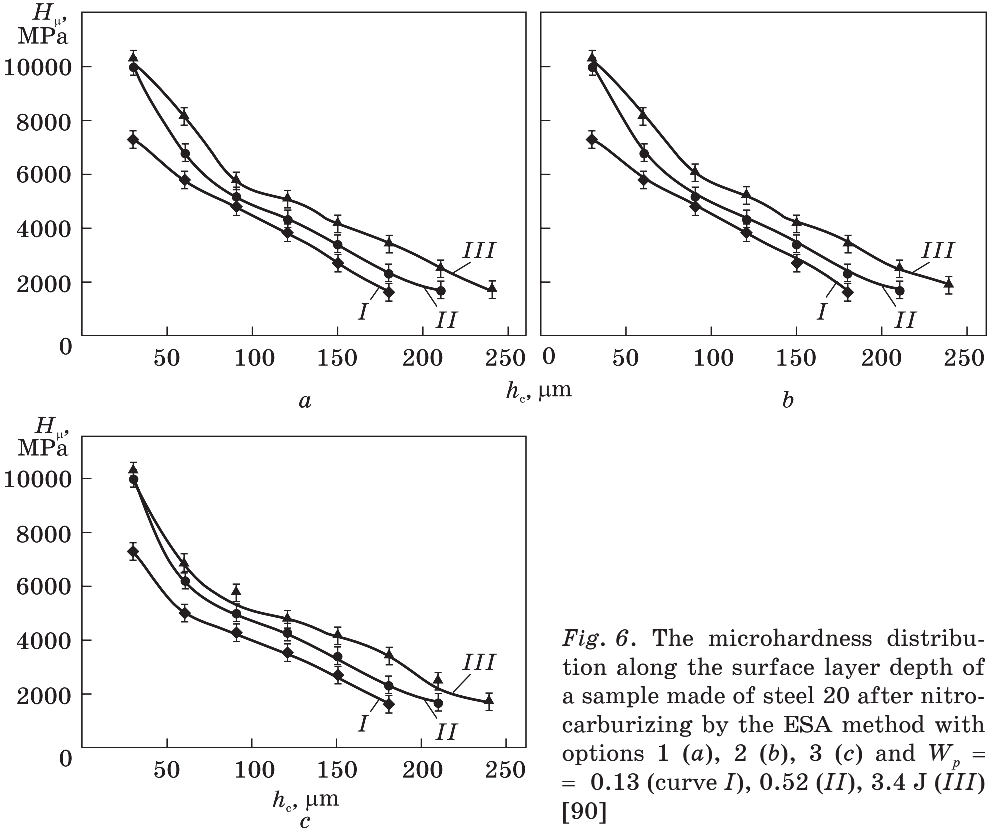

Fig. 6. The microhardness distribution along the surface layer depth of a sample made of steel 20 after nitrocarburizing by the ESA method with options 1 (*a*), 2 (*b*), 3 (*c*) and W_p = = 0.13 (curve *I*), 0.52 (*II*), 3.4 J (*III*) [90]

and 20% petroleum jelly was used to perform the ESC process. The ESA process was carried out at the discharge energies W_p = 0.13, 0.52, and 3.4 J.

There have been investigated microstructures of the steel 20 sample surface layers after nitrocarburizing thereof by the ESA method with the use of the STSM were investigated at different processing productivity levels. The results of the metallographic analysis indicated that the coatings at all productivity levels in Table 4 consisted of three zones, *viz.*, a 'white' layer, a diffusion zone and base metal. The discharge energy and the ESA productivity affect the parameters of the structural zones.

Figure 6 shows the distribution of the microhardness along the depth of the NESC layer on steel 20. It should be noted that the maximum hardness is fixed on the surface and it gradually decreases to the base, the microhardness of which is of 1700–1800 MPa. Gradually changing the microhardness of the coating-base indicates a good adhesion–diffusion bond between the coating and the substrate. The microhardness of the coating zones is determined by the energy parameters of the ESA process: the higher the discharge energy, the higher the hardness of the 'white'

Table 5. **The quality parameters of the steel 20 samples surface layers after nitrocarburizing thereof by the ESA method with the use of the STSM [90]**

Discharge energy, J	Productivity Q, cm^2/min	Labour intensity τ, min/cm^2	Thickness of the strengthened layer, μm	Microhardness, MPa		Roughness R_a, μm	Continuity of the 'white' layer, %
				'white' layer	transition zone		
Existing technology; productivity according to Table 1							
0.13	0.4–0.6	1.7	145–165	7150	4450	1.1	90
0.52	1.0–1.3	0.8	155–190	9921	4650	1.6	100
3.40	1.6–2.2	0.5	210–260	10050	4970	5.9	100
Option 1; the productivity of the ESA is reduced by 2 times (Table 2)							
0.13	0.3	3.3	165–180	7310	4550	1.0	100
0.52	0.6	1.7	175–210	10030	4750	1.5	100
3.40	1.0	1.0	225–275	10250	5130	6.5	100
Option 2; the productivity of the ESA is reduced by 3 times (Table 2)							
0.13	0.2	5.0	170–185	7360	4590	1.0	100
0.52	0.3	3.3	180–215	10090	4780	1.6	100
3.40	0.5	2.0	230–280	10290	5190	6.4	100
Option 3; the productivity of the ESA is reduced by 4 times (Table 2)							
0.13	0.1	10.0	170–185	7360	4530	1.1	100
0.52	0.2	5.0	180–215	10100	4580	1.5	100
3.40	0.3	3.3	230–280	10300	4910	6.3	100

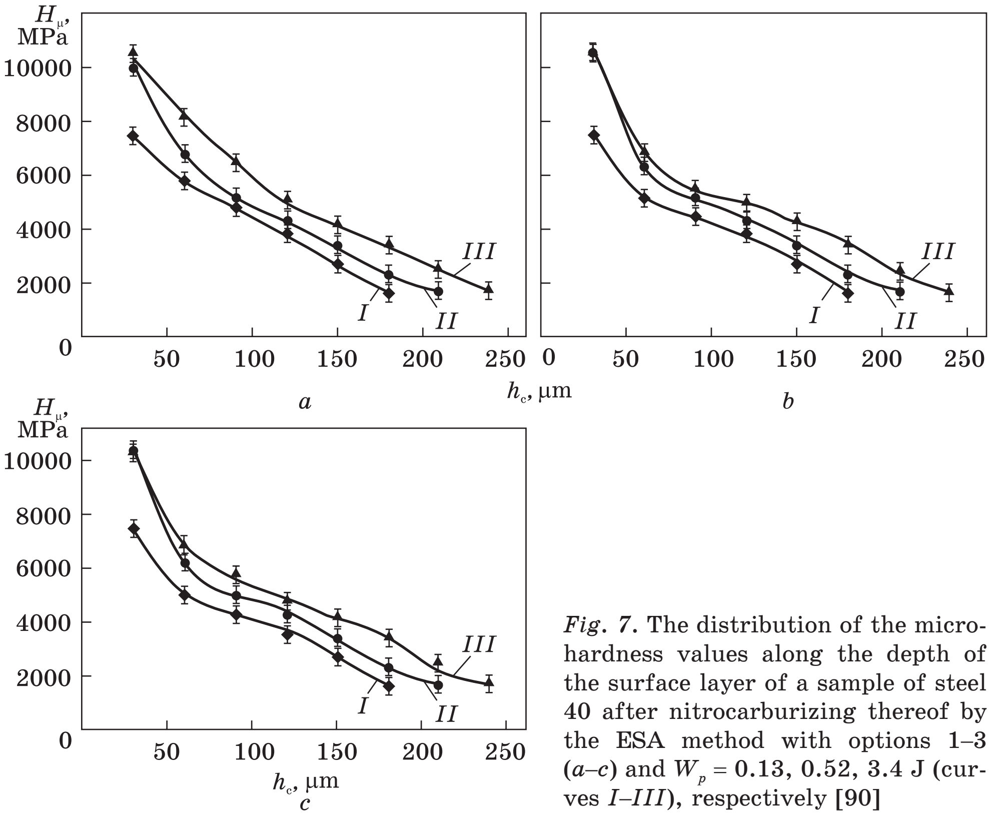

Fig. 7. The distribution of the microhardness values along the depth of the surface layer of a sample of steel 40 after nitrocarburizing thereof by the ESA method with options 1–3 (*a*–*c*) and W_p = 0.13, 0.52, 3.4 J (curves *I*–*III*), respectively [90]

layer and, accordingly, the transition zone. Such a change in microhardness is apparently associated with the diffusion of nitrogen and carbon into the substrate, and it might be caused by a change in the phase composition of the layer [74].

The productivity of the ESA process does not have a significant effect on the microhardness indicators of the strengthened layer, but it has a positive effect on the thickness and continuity of the surface layer in Table 5. If at traditional productivity values (Q = 0.4–0.6 cm^2/min and W_p = 0.13 J), it is not possible to obtain a continuous layer, then, with a decrease in Q, it is possible to achieve 100% continuity with an increase in the thickness of the coating. However, the surface roughness increases.

The analysis of the microstructure of the surface layer of the steel 40 samples after nitrocarburizing by the ESA method using the STSMs containing nitrogen–carbon components was carried out. Due to ESA processing the steel surface, there occurs the ET (anode) destruction; the ET erosion products are transferred to the surface (cathode) being processed, and the micrometallurgical processes occur on the surface being processed;

the ET and the STSM material elements diffuse into the surface layer of the product; the surface of the product acquires a new specific relief; there is formed a modified layer, which contains a 'white' layer and a diffusion zone. Thus, on the surface, a new layer forms with properties different from those of the initial state. Those are determined by the parameters of the spark discharge (discharge energy W_p) and the process productivity (Q).

As on steel 20, increasing the discharge energy increases the thickness of the 'white' layer and that of the diffusion (transition) zone. During the ESA process, with amplification of the discharge energy, the diffusion processes accelerate, and obviously, the diffusion zone between the coating and the base increases. At the classical productivity values in Table 6, at $W_p = 0.13$ J, the thickness of the strengthened layer is 150 to 170 μm, while, at $W_p = 3.4$ J, it is of about 215 to 265 μm. In this case, the continuity of the coating reaches 100%.

Figure 7 shows the microhardness distribution in the surface layer on steel 40. The 'white' layer has a maximum microhardness of 7150 to 10580 MPa, depending on the processing parameters, and it has been gradually decreasing to the hardness of the base. The increase in the hardness of the transition zone can be caused by the phase transformations that occur when the steel has been heated above critical temperatures and rapidly cooled in air. Rapidly cooling after the ESA process leads to some strengthening of the surface layer of the steel and to an increase in hardness. As in steel 20, in the surface layer of steel 40, there is a probability of the formation of intermetallics, nitrides, carbonitrides and oxides since the ESA process has been carried out in air in the STSM environment. In addition, the formation of the above-mentioned phases contributes to an increase in the microhardness of the coating and the diffusion zone.

Figures 8–10 show the dependences of the thickness values of the strengthened layer (a) and the values of microhardness of the 'white' layer on the W_p and τ values when nitrocarburizing by the ESA method of steel 20 for option 1, option 2, and option 3, respectively [92].

It should be noted that, for steel 40, the nature of the dependences of the thickness of the strengthened layer and the microhardness of the 'white' layer on the discharge energy and processing time (labour-intensiveness of the ESA) during the nitrocarburizing process for all processing options in Table 6 does not differ from that of the dependences indicated in Figs. 6–8 for steel 20. A slight difference is noted only in the increase in the thickness of the 'white' layer and microhardness (see Table 5).

Thus, due to the conducted studies, the following conclusions have been achieved:

- compared to nitriding, in the course of the nitrocarburizing process, the thickness of the strengthened surface layer and its microhardness increase;

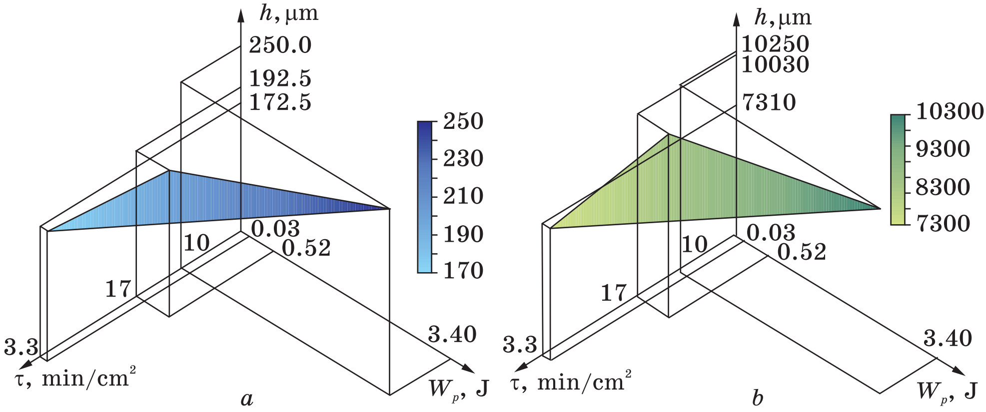

Fig. 8. The dependences of the strengthened layer thickness (*a*) and the microhardness (*b*) of the 'white' layer on W_p and τ during nitrocarburizing the steel 20 for option 1 [92]

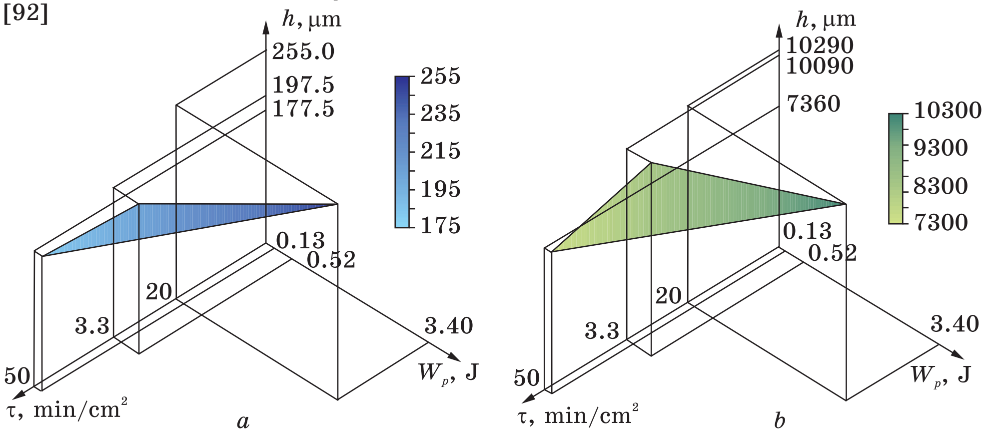

Fig. 9. The same as in the previous figure, but for option 2 [92]

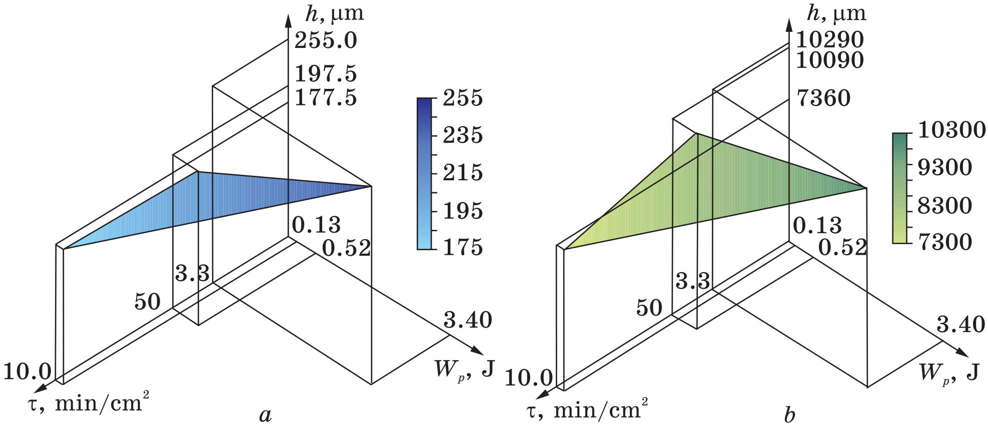

Fig. 10. The same as in the previous figure, but for option 3 [92]

Table 6. **The quality parameters of the steel 40 samples surface layers after nitrocarburizing thereof by the ESA method with the use of the STSM [90]**

Discharge energy, J	Productivity Q, cm^2/min	Labour intensity τ, min/cm^2	Thickness of the strengthened layer, μm	Microhardness, MPa		Roughness R_a, μm	Continuity of the 'white' layer, %
				'white' layer	transition zone		
Existing technology							
0.13	0.4–0.6	1.7	150–170	7150	4450	1.1	90
0.52	1.0–1.3	0.8	160–195	9921	4650	1.6	100
3.40	1.6–2.2	0.5	215–265	10050	4970	5.9	100
Option 1							
0.13	0.3	3.3	170–185	7510	4550	1.0	100
0.52	0.6	1.7	180–215	10520	4750	1.5	100
3.40	1.0	1.0	230–280	10550	5130	6.5	100
Option 2							
0.13	0.2	5.0	175–190	7550	4590	1.0	100
0.52	0.3	3.3	185–220	10560	4780	1.6	100
3.40	0.5	2.0	235–285	10580	5190	6.4	100
Option 3							
0.13	0.1	10.0	175–190	7560	4530	1.1	100
0.52	0.2	5.0	185–220	10560	4580	1.5	100
3.40	0.3	3.3	235–285	10550	4910	6.3	100

• with increasing the discharge energy, the thickness values of the 'white' layer and the diffusion zone also increase, as well as there is an increase in the microhardness, roughness and continuity of the surface;

• with decreasing ESA productivity, the thickness of the strengthened surface layer (zone of increased microhardness) and its microhardness increase, as well as the coating continuity improves;

• when replacing the steel 20 substrate with that made of steel 40, the thickness of the strengthened surface layer and its microhardness slightly increase.

3.2. Determining and Analysing the Quality Parameters of the Part Surfaces Dependent on the Energy and Technological ESA Parameters: STSMs at ESC Processing

According to Ref. [93], the ESC process was carried out in compliance with the following scheme: the samples of steels 20 and 40 had been preliminarily processed by the ESA method with the use of the aluminium ETs at W_p = 3.40 J; then, the carbon-containing STSMs were applied onto to the processed surfaces and subsequently alloyed with the use of the graphite ETs at the productivities according to options 1, 2, and 3 of Table 1, at W_p = 0.13, 0.52, and 3.40 J.

Table 7. **Quality parameters of surface layers of steel 20 samples after carburizing thereof by the ESA method using STSMs [93]**

Discharge energy, J	Productivity Q, cm^2/min	Labour-intensiveness τ, min/cm^2	Thickness of the strengthened layer, μm	Microhardness, MPa		Roughness R_a, μm	Continuity of the 'white' layer, %
				'white' layer	transition zone		
Existing technology							
0.13	0.4–0.6	1.7	145–165	10 370	4450	1.1	90
0.52	1.0–1.3	0.8	155–190	12 050	4650	1.6	100
3.40	1.6–2.2	0.5	210–260	12 200	4970	5.9	100
Option 1							
0.13	0.3	3.3	165–180	10 510	4550	1.0	100
0.52	0.6	1.7	175–210	12 180	4750	1.5	100
3.40	1.0	1.0	225–275	12 290	5130	6.5	100
Option 2							
0.13	0.2	5.0	175–195	10 570	4590	1.0	100
0.52	0.3	3.3	185–220	12 250	4780	1.6	100
3.40	0.5	2.0	235–285	12 330	5190	6.4	100
Option 3							
0.13	0.1	10.0	180–200	10 590	4530	1.1	100
0.52	0.2	5.0	190–225	12 280	4580	1.5	100
3.40	0.3	3.3	240–290	12 350	4910	6.3	100

Due to the metallographic and durometric analyses, as well as the determination of the roughness of the processed surface in Table 7, it has been established as follows.

While carburizing the steel 20 and the steel 40 samples each by the ESA method, a surface layer has been formed, which has a greater thickness of the strengthened zone and higher microhardness as compared to the layer after nitrocarburizing.

With an increase in the discharge energy, the thickness of the strengthened layer and its microhardness, as well as the roughness and continuity of the coating, increase.

With a decrease in the ESA productivity and, accordingly, an increase in the labour-intensiveness of the process, the thickness values of the 'white' layer and the diffusion (transition) zone increase, as well as there is an increase in the microhardness and continuity of the coating;

When replacing steel 20 with steel 40, the thickness of the 'white' layer, the diffusion (transition) zone and the microhardness of the surface increase slightly.

3.3. Mathematical Model for Prediction of the Quality Parameters of the Steel Part Surface Layers: NESC Processing by the ESA

Due to the analysis of Tables 5 and 6, it has been found that, at the existing technology for both steel 20 and steel 40, with an increase in W_p, there is an increase in the thickness of the strengthened layer $\Delta h_{s.l.n.}$ as well as in the microhardness $\Delta H_{s.l.n.}$ of the surface in Table 8. In addition, Table 8 shows that these parameters also increase with the duration of processing a certain plane (τ).

Let us consider the effect of the discharge energy on the thickness of the strengthened layer, $\Delta h_{s.l.n.} = f(W_p)$ [94].

Figures 11, *a* and *b* present the dependences of the thickness of the strengthened layer ($\Delta h_{s.l.n.W_p}$) of steel 20 and steel 40, respectively, at $W_p = 0.13$, 0.52, and 3.4 J and values $1/W_p = 7.7$, 1.9, and 0.3 J^{-1} (in Fig. 12) with the existing technology and the ESA options. Figure 13 presents the dependences of the logarithm of the thickness of the strengthened layer ($\ln\Delta h_{s.l.n.W_p}$) of steel 20 and steel 40 on the value of $1/W_p$.

The analysis of Fig. 13, *a* makes it possible to conclude that there is an exponential relationship between the increase in the thickness of the strengthened layer and the discharge energy (W_p). It has been noted

Table 8. **Dependence of the strengthened layer thickness of steels 20 and 40 and their microhardness on the technological parameters of the ESA process during nitrocarburizing with the use of the STSM [94]**

Discharge energy, J	Productivity Q, cm^2/min	Labour-intensiveness τ, min/cm^2	Thickness $\Delta h_{s.l.n.}$, μm		Microhardness $\Delta H_{s.l.n.}$, MPa	
			Steel 20	Steel 40	Steel 20	Steel 40
Existing technology						
0.13	0.6	1.7	155.0	160.0	7150	7160
0.52	1.2	0.8	170.0	175.0	9921	9950
3.40	2.0	0.5	235.0	240.0	10050	10070
Option 1						
0.13	0.3	3.3	175.0	182.5	7310	7510
0.52	0.6	1.7	190.0	200.0	10030	10520
3.40	1.0	1.0	250.0	255.0	10250	10550
Option 2						
0.13	0.2	5.0	180.0	187.5	7360	7550
0.52	0.3	3.3	200.0	205.0	10090	10560
3.40	0.5	2.0	255.0	262.5	10290	10580
Option 3						
0.13	0.1	10.0	182.5	189.0	7365	7560
0.52	0.2	5.0	202.5	207.5	10100	10565
3.40	0.3	3.3	257.5	265.0	10300	10585

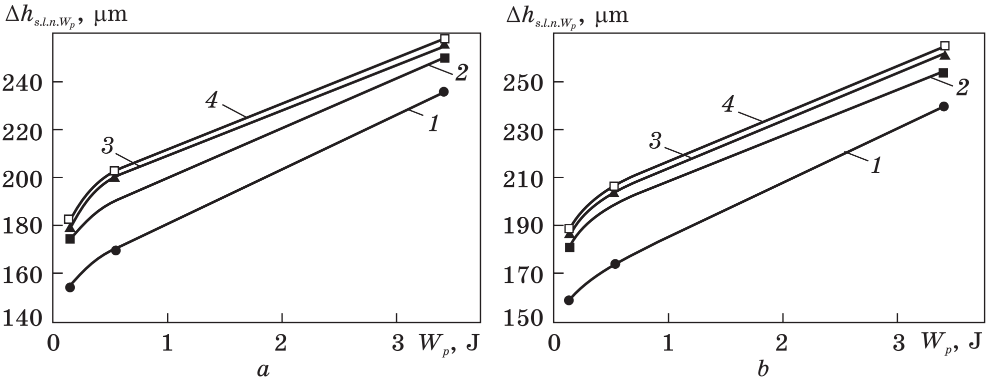

Fig. 11. The strengthened layer thickness $\Delta h_{s.l.n.W_p}$ of steel 20 (*a*) and steel 40 (*b*) *vs*. W_p for existing technology (curve *1*) and ESA options 1–3 (curves *2–4*, respectively) [94]

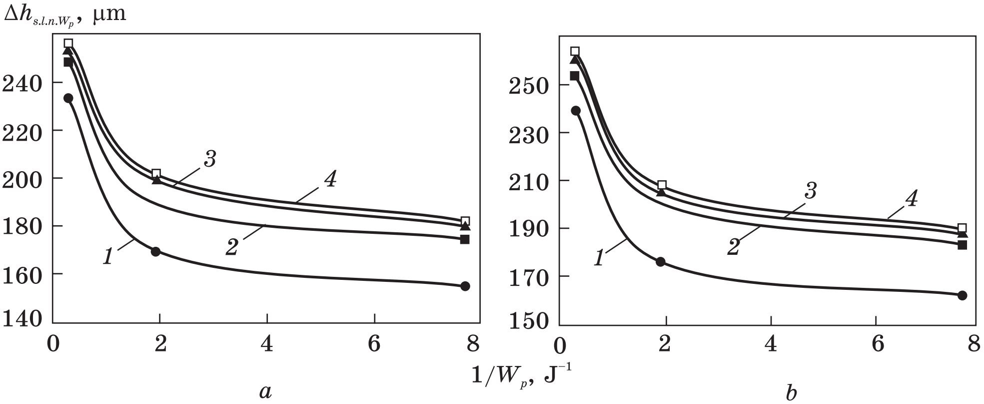

Fig. 12. The same as in the previous figure, but for $\Delta h_{s.l.n.W_p}$ *vs*. $1/W_p$ [94]

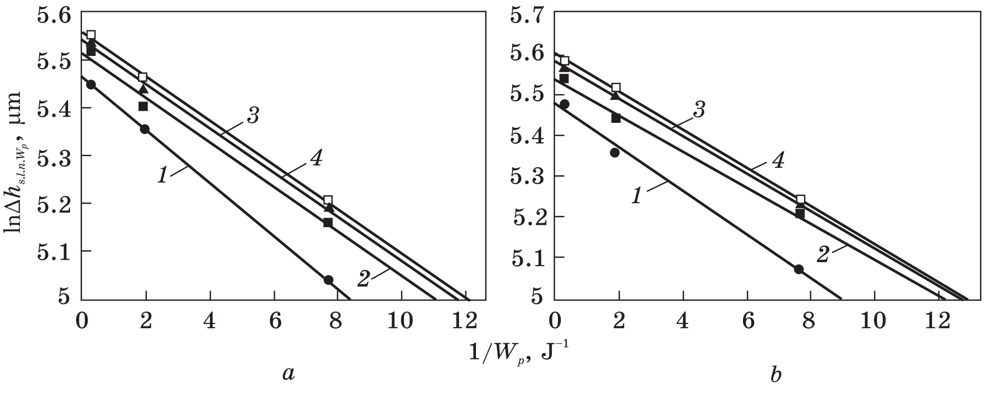

Fig. 13. The same as in the previous figure, but for $\ln \Delta h_{s.l.n.W_p}$ *vs*. $1/W_p$ [94]

that the increase in the thickness of the strengthened layer $\Delta h_{s.l.n.W_p}$ increases with the increase in the activation energy $\Delta E_{\Delta h W_p n.}$ of the nitrocarburizing process.

From the correlation dependence of the increase in the thickness of the strengthened layer on the value of the reciprocal discharge energy (Fig. 12), it follows that (Fig. 13)

$$\ln \Delta h_{s.l.n.W_p} \propto 1/W_p\,,\ \Delta E_{\Delta h W_p n.}\,. \tag{1}$$

Passing from the approximate to the exact equality, we obtain

$$\Delta h_{s.l.n.W_p} = Ce^{\frac{-\Delta E_{\Delta h W_p n.}}{W_p}}\,, \tag{2}$$

where $C = \Delta h_{s.l.n.W_{p\max}}$ ($\Delta h_{s.l.n.W_{p\max}}$ is the greatest thickness of the strengthened layer). Then,

$$\Delta h_{s.l.n.W_p} = \Delta h_{s.l.n.W_{p\max}} e^{\frac{-\Delta E_{\Delta h W_p n.}}{W_p}}\,. \tag{3}$$

Equation (3) can be defined as the equation of the thickness of the strengthened layer depending on the discharge energy. If, in Eq. (3),

$$\Delta E_{\Delta h W_p n.} = W_p\,, \tag{4}$$

$$\Delta h_{s.l.n.W_p} \big/ \Delta h_{s.l.n.W_{p\max}} = e^{-1}\,. \tag{5}$$

Thus, $\Delta E_{\Delta h W_p n.}$ is a physical value that is equal to such a discharge energy W_p, at which the thickness of the strengthened layer is *e* times less than its maximum value.

The $\Delta E_{\Delta h W_p n.}$ value can be determined by the constant of the equation of the thickness of the strengthened layer depending on W_p. The other constant of this equation is $\Delta h_{s.l.n.W_{p\max}}$, *viz.*, the largest thickness of the strengthened layer.

The largest thickness of the strengthened layer $\Delta h_{s.l.n.W_{p\max}}$, *viz.*, the constant of the equation of the strengthened layer thickness, can be determined by the segment cut off on the ordinate axis by the point of intersection of the extended straight line of the graph of the dependence of the logarithm of the thickness of the strengthened layer ($\ln\Delta h_{s.l.n.W_p}$) of steel 20 and steel 40 on the reciprocal value as for the discharge energy, $1/W_p$ (see Fig. 13).

The second constant of the equation of the thickness of the strengthened layer, namely, the activation energy, is denoted as $\Delta E_{\Delta h W_p n.} = \mathrm{tg}\alpha$ where α is the angle of inclination of the straight lines of the dependences of $\ln\Delta h_{s.l.n.W_p}$ on W_p^{-1}.

Let us consider the influence of the labour-intensiveness τ on the change in the thickness of the strengthened layer at the traditional

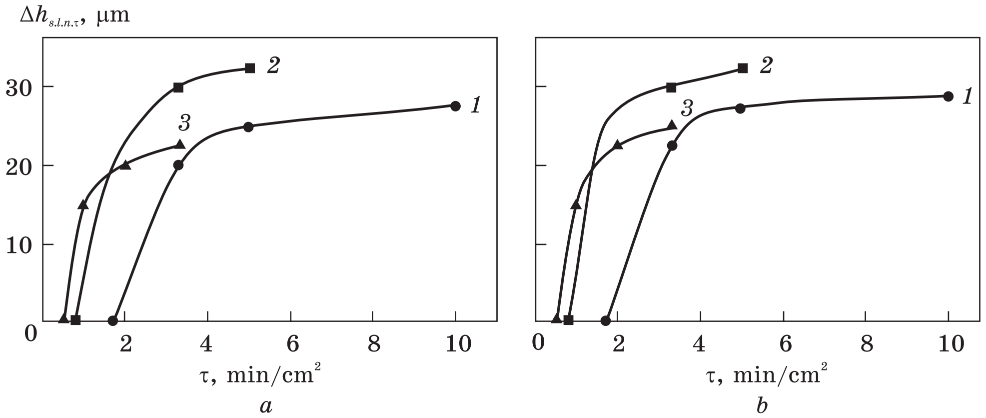

Fig. 14. Graphical representations of the data in Table 9: $\Delta h_{s.l.n.\tau}$ *vs*. τ [94]

Table 9. **The increase in the strengthened layer thickness ($\Delta h_{s.l.n.\tau}$) for different labour-intensiveness values (τ) as a result of the ESA (options 1–3) of steels 20 and 40 at W_p = 0.13, 0.52, 3.4 J [94], as compared with existing technologies, for which $\Delta h_{s.l.n.\tau}$ = 0**

Labour-intensiveness τ, min/cm²	$\Delta h_{s.l.n.\tau}$, μm	Labour-intensiveness τ, min/cm²	$\Delta h_{s.l.n.\tau}$, μm	Labour-intensiveness τ, min/cm²	$\Delta h_{s.l.n.\tau}$, μm
X	Y	*X*	Y	*X*	Y
W_p = 0.13 J		W_p = 0.52 J		W_p = 3.4 J	
Steel 20					
1.7	0	0.8	0	0.5	0
3.3	20.0	1.7	20.0	1.0	15.0
5.0	25.0	3.3	30.0	2.0	20.0
10	27.5	5.0	32.5	3.3	22.5
Steel 40					
1.7	0	0.8	0	0.5	0
3.3	22.5	1.7	25.0	1.0	15.0
5.0	27.5	3.3	30.0	2.0	22.5
10	29.0	5.0	32.5	3.3	25.0

labour-intensiveness of the ESA process and the one being studied, namely, $\Delta h_{s.l.n.} = f(\tau)$. Table 9 and Fig. 14 present the dependences of the increase in the thickness of the strengthened layer of steel 20 and steel 40, respectively, on the labour-intensiveness τ at the existing technology and options 1, 2, and 3 of the ESA process.

Table 10 and Fig. 15 represent the dependences of the increase in the thickness of the strengthened layer ($\Delta h_{s.l.n.\tau}$) for steel 20 and steel 40 on the reciprocal labour-intensiveness, 1/τ, with the existing techno-

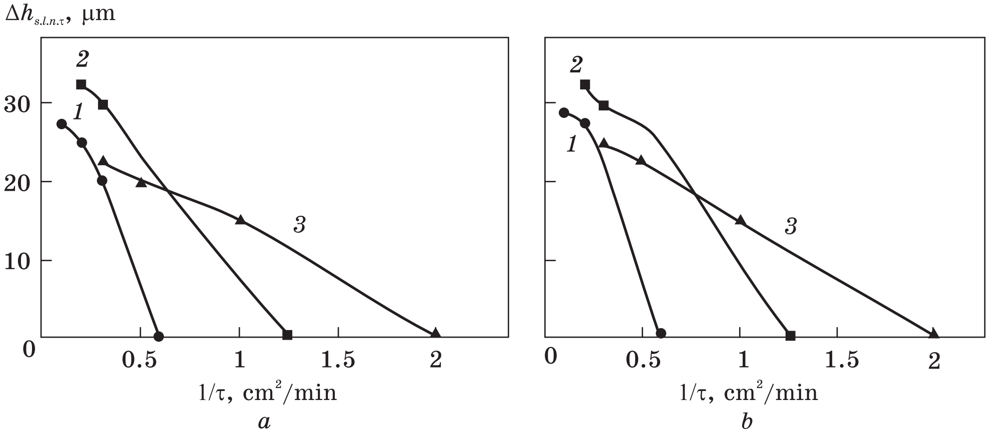

Fig. 15. Graphical view of the data in Table 10: the same as in the previous figure, but for $\Delta h_{s.l.n.\tau}$ *vs*. τ^{-1} [94]

Table 10. **The same as in the previous table, but for different reciprocal labour-intensiveness values τ^{-1} [94]**

Reciprocal labour-intensiveness τ^{-1}, cm²/min	$\Delta h_{s.l.n.\tau}$, μm	Reciprocal labour-intensiveness τ^{-1}, cm²/min	$\Delta h_{s.l.n.\tau}$, μm	Reciprocal labour-intensiveness τ^{-1}, cm²/min	$\Delta h_{s.l.n.\tau}$, μm
X	Y	*X*	Y	*X*	Y
W_p = 0.13 J		W_p = 0.52 J		W_p = 3.4 J	
Steel 20					
0.6	0	1.2	0	2.0	0
0.3	20.0	0.6	20.0	1.0	15.0
0.2	25.0	0.3	30.0	0.5	20.0
0.1	27.5	0.2	32.5	0.3	22.5
Steel 40					
0.6	0	1.2	0	2.0	0
0.3	22.5	0.6	25.0	1.0	15.0
0.2	27.5	0.3	30.0	0.5	22.5
0.1	29.0	0.2	32.5	0.3	25.0

logy and options 1, 2, and 3 of the ESA process. Table 11 and Fig. 16 represent the dependences of the logarithm of the increase in the thickness of the strengthened layer ($\Delta E_{\Delta hW_pn.}$) for steel 20 and steel 40 on the reciprocal labour-intensiveness (1/τ).

The analysis of Fig. 16 makes it possible to conclude that there is an exponential relationship between the increase $\Delta h_{s.l.n.\tau}$ and the labour-intensiveness τ. It has been noted that the increase in the thickness of the strengthened layer $\Delta h_{s.l.n.W_p}$ grows with the increase in the activation energy $\Delta E_{\Delta hW_pn.}$ of the nitrocarburizing process.

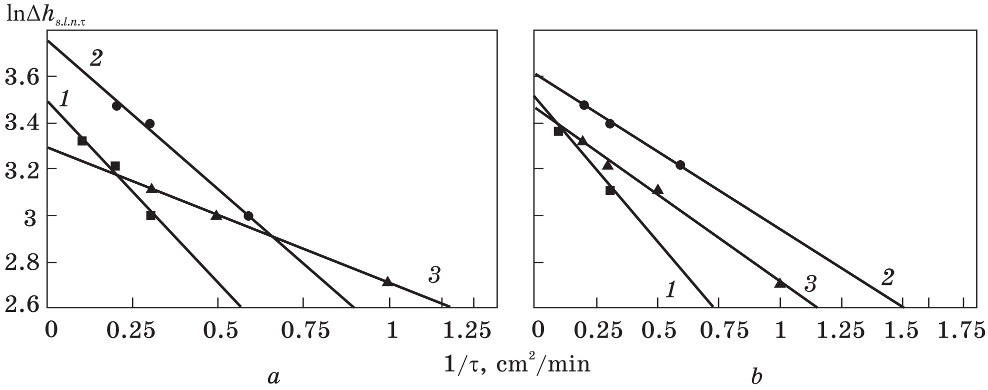

Fig. 16. Graphical visualisations of the data in Table 11: the same as in the previous figure, but for $\ln\Delta h_{s.l.n.\tau}$ *vs*. τ^{-1} [94]

Table 11. **The same as in the previous table, but logarithmic values of the strengthened layer thickness ($\ln\Delta h_{s.l.n.\tau}$) for different reciprocal labour-intensiveness values (τ^{-1}) [94]**

Reciprocal labour-intensiveness τ^{-1}, cm²/min	$\ln\Delta h_{s.l.n.\tau}$	Reciprocal labour-intensiveness τ^{-1}, cm²/min	$\ln\Delta h_{s.l.n.\tau}$	Reciprocal labour-intensiveness τ^{-1}, cm²/min	$\ln\Delta h_{s.l.n.\tau}$
X	*Y*	*X*	*Y*	*X*	*Y*
$W_p = 0.13$ J		$W_p = 0.52$ J		$W_p = 3.4$ J	
Steel 20					
0.3	2.99	0.6	2.99	2	2.70
0.2	3.22	0.3	3.40	1	2.99
0.1	3.31	0.2	3.48	0.5	3.11
Steel 40					
0.3	3.11	0.6	3.22	2	2.70
0.2	3.31	0.3	3.40	1	3.11
0.1	3.37	0.2	3.48	0.5	3.22

From the correlation dependence of the increase in the thickness of the strengthened layer on the reciprocal labour-intensiveness value (see Fig. 15), it follows that the logarithm of the increase in the thickness of the strengthened layer (Fig. 16)

$$\ln\Delta h_{s.l.n.\tau} \propto -\tau^{-1}. \tag{6}$$

Running from the approximate to the exact equality, we have

$$\Delta h_{s.l.n.\tau} = C_1 e^{\frac{-1}{\tau}}, \tag{7}$$

where $C_1 = \Delta h_{s.l.n.\tau_{\max}}$, $\Delta h_{s.l.n.\tau_{\max}}$ is the largest increase in the thickness of the strengthened layer:

$$\Delta h_{s.l.n.\tau} = \Delta h_{s.l.n.\tau_{\max}} e^{\frac{-1}{\tau}} . \quad (8)$$

Dependence (8) can be considered as an equation of the increase in the thickness of the strengthened layer depending on the labour-intensiveness. The largest thickness of the strengthened layer $\Delta h_{s.l.n.\tau_{\max}}$, that is the constant of the equation of the increase in the thickness of the strengthened layer depending on the labour-intensiveness, can be determined by the value of the segment cut off on the ordinate axis by the point of intersection of the extended straight line of the graph of the dependence ($\ln \Delta h_{s.l.n.\tau}$) of steel 20 and steel 40 on $1/\tau$ (Fig. 16).

Considering that the total increase in the thickness of the layer of increased hardness depends on W_p and labour-intensiveness, *i.e.*, $\sum \Delta h_{s.l.n.} = f(W_p, \tau)$ after the above studies, it can be concluded that

$$\sum \Delta h_{s.l.n.} = \Delta h_{s.l.n.W_{p\max}} e^{\frac{-\Delta E_{\Delta h W_p n.}}{W_p}} + \Delta h_{s.l.n.\tau_{\max}} e^{\frac{-1}{\tau}} . \quad (9)$$

Dependence (9) can be taken into account by the equation of the total increase in the thickness of the strengthened layer.

Further, we consider the effect of the discharge energy on the microhardness of the strengthened layer in the course of the nitrocarburization process. The dependences of the microhardness of the strengthened layer ($\Delta H_{\mu_{s.l.n.W_p}}$) of steel 20 and steel 40 on the W_p = 0.13, 0.52, 3.4 J are shown in Fig. 17, and, on the $1/W_p$ = 7.7, 1.9, 0.3 1/J, they are shown in Fig. 18 with existing nitrocarburizing technology (*1*) and options *1*, *2*, *3* of the ESA process (*2*)–(*4*).

Figure 19 presents the dependences of the logarithm of the microhardness of the strengthened layer $\ln \Delta H_{\mu_{s.l.n.W_p}}$ of steel 20 and steel 40 on $1/W_p$.

The analysis of Fig. 17 has shown that there is an exponential relationship between the increase in the microhardness of the strengthened layer and the discharge energy (W_p). It has been noted that the increase in the microhardness of the strengthened layer increases with an increase in the activation energy of the nitrocarburizing process ($\Delta E_{\Delta H_\mu W_p n.}$).

From the correlation dependence of the increase in the microhardness of the strengthened layer on the reciprocal discharge energy (Fig. 18), it follows that the logarithm of the microhardness of the strengthened layer and the activation energy:

$$\ln \Delta H_{\mu_{s.l.n.W_p}} \propto 1/W_p , \Delta E_{\Delta H_\mu W_p n.}. \quad (10)$$

Proceeding from the approximate to the exact equality, we obtain

$$\Delta H_{\mu_{s.l.n.W_p}} = C_2 e^{\frac{-E_{\Delta H_\mu W_p n.}}{W_p}} , \quad (11)$$

where $C_2 = \Delta H_{\mu_{s.l.n.W_{p\max}}}$ ($\Delta H_{\mu_{s.l.n.W_{p\max}}}$ is the greatest thickness of the streng-

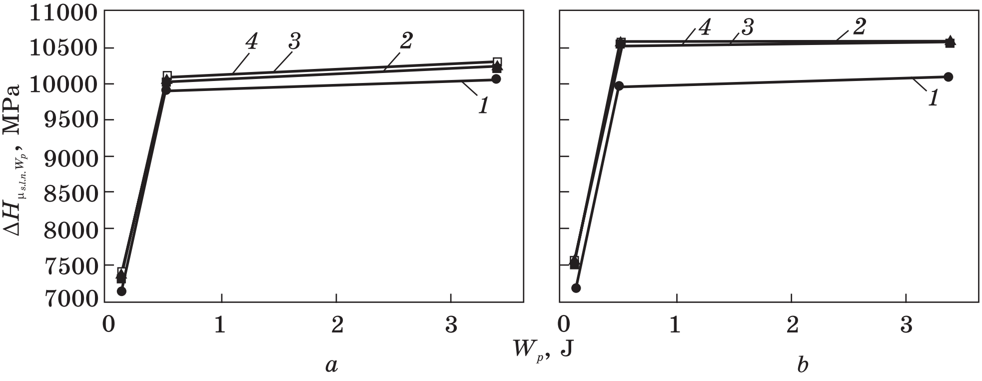

Fig. 17. Microhardness of the strengthened layer ($\Delta H_{\mu_{s.l.n.W_p}}$) *vs*. W_p for steels 20 (*a*) and 40 (*b*), where curve *1* corresponds to the existing technology, while curves *2–4* — options 1–3, respectively, of the ESA process [94]

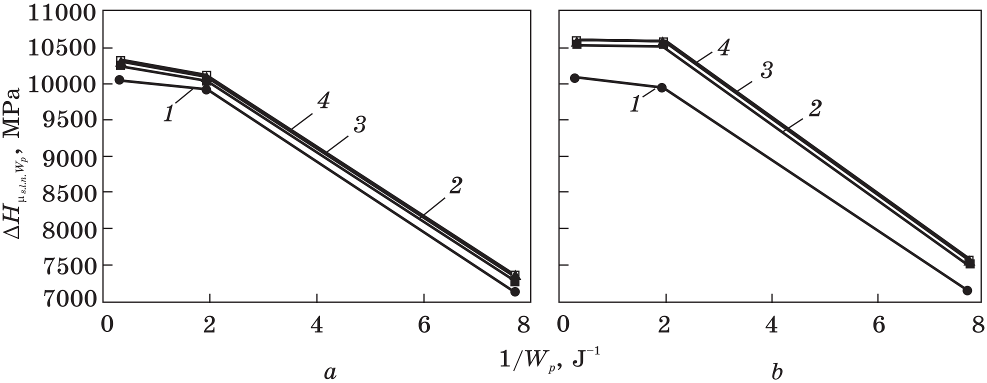

Fig. 18. The same as in previous figure, but for $\Delta H_{\mu_{s.l.n.W_p}} = \Delta H_{\mu_{s.l.n.W_p}}(1/W_p)$ [94]

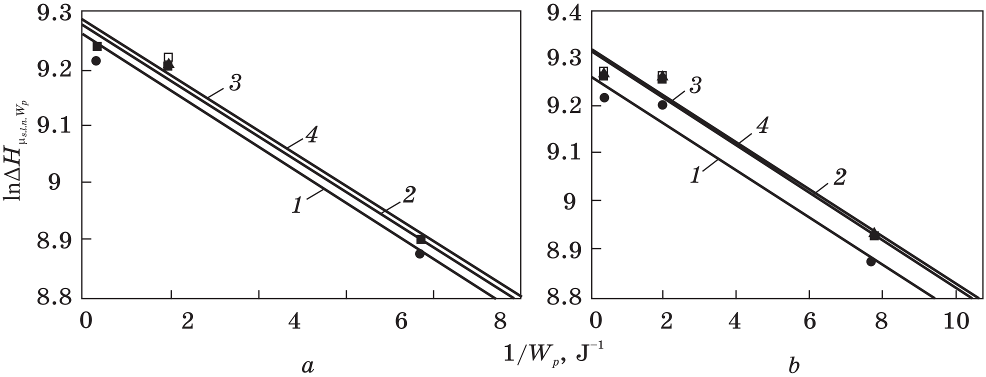

Fig. 19. The same as in the previous figure, but the dependence is logarithmic: $\ln\Delta H_{\mu_{s.l.n.W_p}}$ *vs*. $1/W_p$ [94]

thened layer). Then,

$$\Delta H_{\mu_{s.l.n.W_p}} = \Delta H_{\mu_{s.l.n.W_{p\max}}} e^{\frac{-E_{\Delta H_\mu W_p n.}}{W_p}} . \quad (12)$$

The latter dependence (12) can be taken into account by the equation of the total increase in the thickness of the strengthened layer.

Dependence (12) can be defined as the equation of the microhardness of the strengthened layer depending on the discharge energy. If, in Eq. (12),

$$E_{\Delta H_\mu W_p n.} = W_p , \quad (13)$$

$$\Delta H_{\mu_{s.l.n.W_p}} \Big/ \Delta H_{\mu_{s.l.n.W_{p\max}}} = e^{-1} . \quad (14)$$

Thus, the activation energy $\Delta E_{\Delta H_\mu W_p n.}$ is a physical value that is equal to the discharge energy W_p, at which the microhardness of the strengthened layer is e times less than its maximum value.

The value of $\Delta E_{\Delta H_\mu W_p n.}$ can be determined as a constant of the equation of the microhardness of the strengthened layer depending on W_p. The other constant of this equation is $\Delta H_{\mu_{s.l.n.}W_{p\max}}$, *viz.*, the greatest microhardness of the strengthened layer.

The greatest microhardness of the strengthened layer $\Delta H_{\mu_{s.l.n.}W_{p\max}}$, namely, the constant of the equation of the thickness of the strengthened layer, can be found by the segment cut off on the ordinate axis by the straight line of the dependence of the logarithm of the microhardness of the strengthened layer ($\ln \Delta H_{\mu_{s.l.n.}W_p}$) of steel 20 and steel 40 on the reciprocal discharge energy $1/W_p$ (in Fig. 19). The other constant of the equation of the thickness of the strengthened layer is defined as $\Delta E_{\Delta H_\mu W_p n.} = \mathrm{tg}\alpha$, where α is an angle of the inclination of the straight lines of the dependences $\ln \Delta H_{\mu_{s.l.n.}W_p}$ on $1/W_p$.

Let us consider the influence of the labour-intensiveness τ on the increase in the microhardness of the strengthened layer, $\Delta H_{s.l.n.} = f(\tau)$. Table 12 and Fig. 20 here represent the dependences of the increase in the microhardness of the strengthened layer ($\Delta H_{\mu_{s.l.n.\tau}}$) of steel 20 and steel 40 each on the labour-intensiveness τ for the existing technology and options 1, 2, and 3 of the ESA process at the W_p = 0.13, 0.52, and 3.4 J.

Analysing Fig. 20 allows us to conclude that there is an exponential relationship between the increase in the microhardness of the strengthened layer ($\Delta H_{\mu_{s.l.n.\tau}}$) and the labour-intensiveness τ. The increase in the microhardness of the strengthened layer $\Delta H_{\mu_{s.l.n.\tau}}$ increases with increasing τ.

Table 13 and Fig. 21 represent the dependences of the increase in $\Delta H_{\mu_{s.l.n.\tau}}$ for steel 20 and steel 40 on the values of $1/\tau$. Those are given for the existing technology and options 1, 2, and 3 of the ESA process.

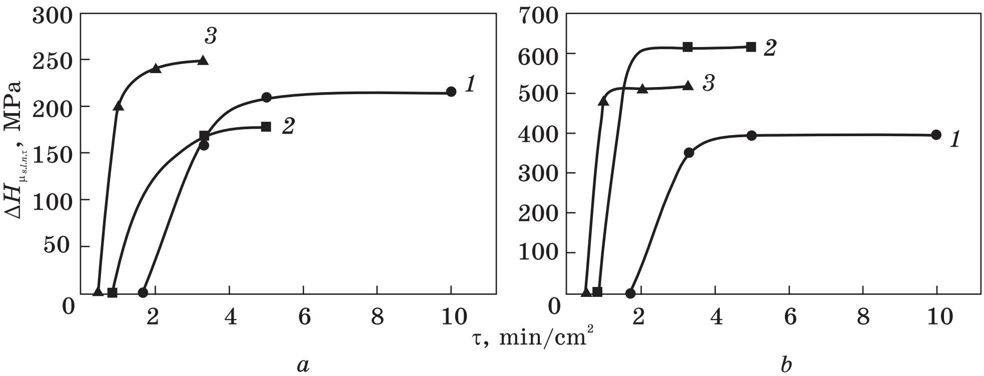

Fig. 20. Graphical representation of the data in Table 12: $\Delta H_{\mu_{s.l.n.\tau}}$ *vs*. τ [94]

Table 12. **The increase in the strengthened layer microhardness ($\Delta H_{\mu_{s.l.n.\tau}}$) for different labour-intensiveness values (τ) due to the ESA (options 1–3) of steels 20 and 40 at W_p = 0.13, 0.52, 3.4 J [94] as compared with existing technologies**

Labour-intensiveness τ, cm²/min	$\Delta H_{\mu_{s.l.n.\tau}}$, MPa	Labour-intensiveness τ, cm²/min	$\Delta H_{\mu_{s.l.n.\tau}}$, MPa	Labour-intensiveness τ, cm²/min	$\Delta H_{\mu_{s.l.n.\tau}}$, MPa
X	*Y*	*X*	*Y*	*X*	*Y*
W_p = 0.13 J		W_p = 0.52 J		W_p = 3.4 J	
Steel 20					
1.7	0	0.8	0	0.5	0
3.3	160	1.7	109	1.0	200
5.0	210	3.3	169	2.0	240
10	215	5.0	179	3.3	250
Steel 40					
1.7	0	0.8	0	0.5	0
3.3	350	1.7	570	1.0	480
5.0	390	3.3	610	2.0	510
10	400	5.0	615	3.3	518

Table 14 and Fig. 22 represent the dependences $\ln \Delta H_{\mu_{s.l.n.\tau}}$ for steels 20 and 40 on the values with the reciprocal labour-intensiveness (1/τ).

As follows from the correlation dependence of the increase in the microhardness of the strengthened layer on the reciprocal labour-intensiveness (Fig. 20), the logarithm of the increase in the microhardness of the strengthened layer (Fig. 21),

$$\ln \Delta H_{\mu_{s.l.n.\tau}} \propto \tau^{-1}. \quad (15)$$

Running from the approximate equality to the exact one, we have

$$\Delta H_{\mu_{s.l.n.\tau}} = C_3 e^{\frac{-1}{\tau}}, \quad (16)$$

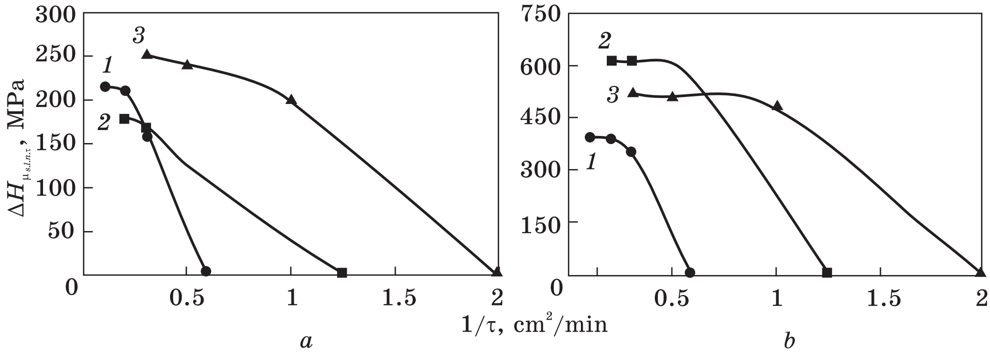

Fig. 21. Graphical view of the data in Table 13: the same as in the previous figure, but for $\Delta H_{\mu_{s.l.n.\tau}}$ *vs*. τ^{-1} [94]

Table 13. **The same as in the previous table, but for different reciprocal labour-intensiveness values (τ^{-1}) [94]**

Reciprocal labour-intensiveness 1/τ, cm²/min	$\Delta H_{\mu_{s.l.n.\tau}}$, MPa	Reciprocal labour-intensiveness 1/τ, cm²/min	$\Delta H_{\mu_{s.l.n.\tau}}$, MPa	Reciprocal labour-intensiveness 1/τ, cm²/min	$\Delta H_{\mu_{s.l.n.\tau}}$, MPa
X	*Y*	*X*	*Y*	*X*	*Y*
W_p = 0.13 J		W_p = 0.52 J		W_p = 3.4 J	
Steel 20					
0.6	0	1.2	0	2.0	0
0.3	160	0.6	109	1.0	200
0.2	210	0.3	169	0.5	240
0.1	215	0.2	179	0.3	250
Steel 40					
0.6	0	1.2	0	2.0	0
0.3	350	0.6	570	1.0	480
0.2	390	0.3	610	0.5	510
0.1	400	0.2	615	0.3	518

where $C_3 = \Delta H_{\mu_{s.l.n.\tau_{max}}}$; $\Delta H_{\mu_{s.l.n.\tau_{max}}}$ is the greatest increase in the microhardness of the strengthened layer. Then,

$$\Delta H_{\mu_{s.l.n.\tau}} = \Delta H_{\mu_{s.l.n.\tau_{max}}} e^{\frac{-1}{\tau}}. \tag{17}$$

Dependence (17) can be considered as an equation of the increase in the microhardness of the strengthened layer depending on the labour-intensiveness.

The greatest increase in the microhardness of the strengthened layer $\Delta H_{\mu_{s.l.n.\tau_{max}}}$, that is the constant of the equation of the increase in the microhardness of the strengthened layer depending on the labour-intensiveness, can be determined with the value of the segment

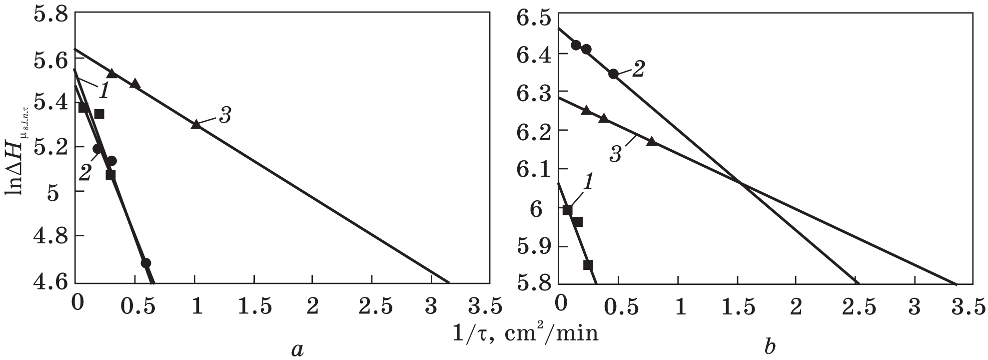

Fig. 22. The dependence of $\ln\Delta H_{\mu_{s.l.n.\tau}}$ on τ^{-1} for the existing technology and all the options of the ESA of steels 20 (*a*) and 40 (*b*), where W_p = 0.13 (curve *1*), 0.52 (curve *2*), and 3.4 J (curve *3*) [94]

Table 14. **The same as in the previous table, but for $\ln\Delta H_{\mu_{s.l.n.\tau}}$ *vs.* τ^{-1} [94]**

Reciprocal labour-intensiveness τ^{-1}, cm²/min	$\ln\Delta H_{\mu_{s.l.n.\tau}}$	Reciprocal labour-intensiveness τ^{-1}, cm²/min	$\ln\Delta H_{\mu_{s.l.n.\tau}}$	Reciprocal labour-intensiveness τ^{-1}, cm²/min	$\ln\Delta H_{\mu_{s.l.n.\tau}}$
X	*Y*	*X*	*Y*	*X*	*Y*
W_p = 0.13 J		W_p = 0.52 J		W_p = 3.4 J	
Steel 20					
0.3	5.08	0.6	4.69	1	5.30
0.2	5.35	0.3	5.13	0.5	5.48
0.1	5.37	0.2	5.19	0.3	5.52
Steel 40					
0.3	5.86	0.6	6.35	1	6.17
0.2	5.97	0.3	6.41	0.5	6.23
0.1	5.99	0.2	6.42	0.3	6.25

cut off on the ordinate axis by the point of the intersection of the extended straight line of the graph of the dependence of the logarithm of the increase in the microhardness of the strengthened layer ($\ln\Delta H_{\mu_{s.l.n.\tau}}$) of steels 20 and 40 on the reciprocal labour-intensiveness $1/\tau$ (Fig. 22).

Considering that the total increase in the microhardness of the strengthened layer depends on the discharge energy and labour-intensiveness, that is $\sum\Delta H_{\mu_{s.l.n.}} = f(W_p, \tau)$ after the above studies, it can be concluded that

$$\sum \Delta H_{\mu_{s.l.n.}} = \Delta H_{\mu_{s.l.n.W_{p\max}}} e^{\frac{-E_{\Delta H_\mu W_p n.}}{W_p}} + \Delta H_{\mu_{s.l.n.\tau_{\max}}} e^{\frac{-1}{\tau}}. \quad (18)$$

Dependence (18) can be considered as an equation of the increase in the microhardness of the strengthened layer depending on the ESA process parameters.

Table 15 presents the summarised data in compliance with the constants of the equations of the thickness of the strengthened layer and its microhardness in the course of the nitrocarburization of steels 20 and 40 using the ESA method.

In conclusion to this subsection, we can summarize as follows.

There have been developed the mathematical models of the dependences of the surface quality values during the NESC process by the ESA method with the use of the STSMs (the equation of the increase in the thickness of the strengthened layer and the equation of the increase in the microhardness of the surface) on the energy and the technological parameters of the ESA equipment: the discharge energy (W_p) and the labour-intensiveness (τ), respectively. This event allows determining the main technological parameters of the formed layers, namely, the values of the thickness of the strengthened layers $h_{s.l.n.}$ and those of the microhardness $H_{\mu_{s.l.n.}}$ thereof.

There has been set a method for determining the constants of the equation for the increase in the thickness of the strengthened layer (the greatest increase in the thickness of the strengthened layer depending on the discharge energy $\Delta h_{s.l.n.W_{p\max}}$, activation energy $\Delta E_{\Delta hW_pn.}$ and the greatest increase in the thickness of the strengthened layer depending on the labour-intensiveness of ESA processing $\Delta h_{s.l.n.\tau_{\max}}$, as well as the equation for the increase in the microhardness of the surface (the greatest increase

Table 15. **The constants of equations of the thickness of the strengthened layer and its microhardness in the course of the process of nitrocarburizing steels 20 and 40 using the ESA method [94]. Here, the numerator is the value of the constants for steel 20; the denominator is that for steel 40**

ESA modes	$\Delta h_{s.l.n.W_{p\max}}$, μm	$\Delta E_{\Delta hW_pn.}$ as tgα	$\Delta h_{s.l.n.\tau_{\max}}$, μm	$\Delta H_{\mu s.l.n.W_{p\max}}$, MPa	$\Delta E_{\Delta H_\mu W_pn.}$ as tgα	$\Delta H_{\mu s.l.n.\tau_{\max}}$, MPa
Existing modes	236.8 / 240.2	0.710 / 0.713	—	10498 / 10524	1.204 / 1.204	—
Option 1	248.4 / 254.9	0.717 / 0.720	32.9 / 33.7	10657 / 11109	1.206 / 1.210	259.5 / 433.2
Option 2	255.5 / 266.5	0.720 / 0.726	42.0 / 37.0	10705 / 11110	1.207 / 1.210	241.7 / 644.2
Option 3	259.1 / 270.5	0.722 / 0.728	26.8 / 31.9	10716 / 11100	1.207 / 1.211	279.0 / 537.2

in the microhardness of the strengthened layer depending on the discharge energy $\Delta H_{\mu_{s.l.n.W_p}}$, activation energy $\Delta E_{\Delta H_\mu W_p n.}$, and the greatest increase in the microhardness of the strengthened layer depending on the labour-intensiveness of ESA processing $\Delta H_{\mu_{s.l.n.\tau}}$).

3.4. Mathematical Model for Predicting the Quality Parameters of the Steel-Part Surface Layers: ESC Processing by the ESA

The carried out investigations allow setting the correlations between the energy and technological parameters of the equipment for the ESC: W_p and τ, respectively, and the main parameters of the quality of the surface layers, namely, the thickness of the strengthened layer ($h_{s.l.c.}$) and the microhardness of the surface carburized by the ESA method ($H_{s.l.c.}$).

The previous studies in Table 7 have shown that, with the existing technology for both steel 20 and steel 40, with an increase in W_p, the thickness of the strengthened layer ($\Delta h_{s.l.c.}$) increases, which consists of the thickness of the 'white' layer and the diffusion zone, as well as the microhardness ($\Delta H_{\mu_{s.l.c.}}$) of the surface (Table 16). In addition, Table 16 shows that these parameters also increase with the duration of processing a certain plane (τ). Here, it is a consideration of the effect of the

Table 16. **The dependence of the thickness of the strengthened layer and its microhardness on the technological parameters of the ESA process, while carburizing with the use of the STSMs [94]**

Discharge energy W_p, J	Productivity Q, cm²/min	Labour-intensiveness τ, min/cm²	Thickness of the strengthened layer $\Delta h_{s.l.c.}$, μm		Microhardness of the strengthened layer $\Delta H_{\mu_{s.l.c.}}$, MPa	
			Steel 20	Steel 40	Steel 20	Steel 40
	Existing technology					
0.13	0.6	1.7	155.0	160.0	10370	11760
0.52	1.2	0.8	172.5	177.5	12050	12240
3.40	2.0	0.5	235.0	240.0	12200	12375
	Option 1					
0.13	0.3	3.3	172.5	175.0	10510	11880
0.52	0.6	1.7	192.5	195.5	12130	12360
3.40	1.0	1.0	250.0	255.0	12290	12490
	Option 2					
0.13	0.2	5.0	180.0	185.0	10570	11930
0.52	0.3	3.3	200.0	207.5	12250	12415
3.40	0.5	2.0	255.0	265.0	12330	12540
	Option 3					
0.13	0.1	10.0	182.5	190.0	10590	11950
0.52	0.2	5.0	202.5	210.5	12280	12435
3.40	0.3	3.3	257.5	270.0	12350	12555

discharge energy on the thickness of the strengthened layer, namely, $\Delta h_{s.l.c.} = f(W_p)$.

The methodology of the research aimed at setting the dependences between the energy and technological parameters of the equipment during the ESC process (W_p and τ, respectively) and the main parameters of the quality of the surface layers, namely, the thickness of the strengthened layer ($\Delta h_{s.l.c.}$) and the microhardness of the surface carburized by the ESA method ($\Delta H_{\mu_{s.l.c.}}$), coincides with the methodology for predicting these parameters, which have been presented above. Therefore, we would focus only on the theoretical investigations without references to the experimental studies [94].

From the correlation dependence of the thickness of the strengthened layer on the reciprocal discharge energy, it follows that

$$\ln \Delta h_{s.l.c.W_p} \propto 1/W_p,\ \Delta E_{\Delta h W_p c.}. \tag{19}$$

On the way from the approximate to equality, we obtain

$$\Delta h_{s.l.c.W_p} = C_4 e^{\frac{-\Delta E_{\Delta h W_p c.}}{W_p}}, \tag{20}$$

where $C_4 = \Delta h_{s.l.c.W_{p\max}}$; $\Delta h_{s.l.c.W_{p\max}}$ is the greatest thickness of the strengthened layer. Then,

$$\Delta h_{s.l.c.W_p} = \Delta h_{s.l.c.W_{p\max}} e^{\frac{-\Delta E_{\Delta h W_p c.}}{W_p}}. \tag{21}$$

Dependence (21) can be considered as an equation of the thickness of the strengthened layer depending on the discharge energy.

If

$$\Delta E_{\Delta h W_p c.} = W_p, \tag{22}$$

$$\Delta h_{s.l.c.W_p} \Big/ \Delta h_{s.l.c.W_{p\max}} = e^{-1}. \tag{23}$$

Thus, the activation energy $\Delta E_{\Delta h W_p c.}$ is a physical value equal to the discharge energy W_p, at which the thickness of the strengthened layer is *e* times less than its maximum value. The value $\Delta E_{\Delta h W_p c.}$ can be determined by the constant of the equation of the thickness of the strengthened layer depending on the discharge energy. The other constant of this equation is $\Delta h_{s.l.c.W_{p\max}}$, *i.e.*, the greatest thickness of the strengthened layer.

The greatest thickness of the strengthened layer $\Delta h_{s.l.c.W_{p\max}}$, *viz.*, the constant of the equation of the thickness of the strengthened layer, can be determined by the value of the segment cut-off on the ordinate axis by the point of intersection of the extended straight line of the graph of the dependence of the logarithm of the thickness of the strengthened layer ($\ln \Delta h_{s.l.c.W_p}$) of steels 20 and 40 on the reciprocal discharge energy $1/W_p$. The other constant of the equation for the thickness of the strengthened layer, the activation energy, is defined as $\Delta E_{\Delta h W_p c.} = \text{tg}\alpha$, where α is the angle of inclination of the straight lines of the dependences of $\ln\Delta h_{s.l.c.W_p}$ on $1/W_p$.

Let us consider the influence of the labour-intensiveness, τ, on the change in the thickness of the strengthened layer at the existing labour intensity of the CESA process and the one being studied, *viz.*, $\Delta h_{s.l.c.} = f(\tau)$.

As follows from the correlation dependence of the thickness increase of the strengthened layer on the reciprocal discharge energy value, the logarithm of the thickness increase of the strengthened layer is

$$\ln\Delta h_{s.l.c.\tau} \propto -\tau^{-1} . \tag{24}$$

Taking the exact equality instead of the approximate one, we obtain

$$\Delta h_{s.l.c.\tau} = C_5 e^{\frac{-1}{\tau}} , \tag{25}$$

where $C_5 = \Delta h_{s.l.c.\tau_{\max}}$ ($\Delta h_{s.l.c.\tau_{\max}}$ is the greatest thickness increase of the strengthened layer) and

$$\Delta h_{s.l.c.\tau} = \Delta h_{s.l.c.\tau_{\max}} e^{\frac{-1}{\tau}} . \tag{26}$$

Relation (26) can be considered as an equation of the increase in the thickness of the strengthened layer depending on the labour-intensiveness. The greatest thickness of the strengthened layer, the constant of the equation of the increase in the thickness of the strengthened layer depending on the labour-intensiveness, can be determined by the value of the segment cut off on the ordinate axis by the point of intersection of the extended straight line of the graph of the dependence of the logarithm of the increase in the thickness of the strengthened layer ($\ln\Delta h_{s.l.c.\tau}$) of steel 20 and steel 40 on the labour-intensiveness reciprocal value ($1/\tau$).

Considering that the total increase in the thickness of the strengthened layer depends on the discharge energy and labour-intensiveness, $\sum\Delta h_{\mu_{s.l.c.}} = f(W_p, \tau)$, after the above studies, it is quite possible to conclude that

$$\sum\Delta h_{s.l.c.} = \Delta h_{s.l.c.W_{p\max}} e^{\frac{-\Delta E_{\Delta h W_p c.}}{W_p}} + \Delta h_{s.l.c.\tau_{\max}} e^{\frac{-1}{\tau}} . \tag{27}$$

Expression (27) can be taken into account by the equation for the total increase in the thickness of the strengthened layer.

Further, we consider the effect of the discharge energy on the microhardness of the strengthened layer: $\Delta H_{\mu_{s.l.c.}W_p} = f(W_p)$.

As follows from the correlation dependence of the microhardness of the strengthened layer on the value of the reciprocal discharge energy,

$$\ln \Delta H_{\mu_{s.l.c.W_p}} \propto 1/W_p\,,\ \Delta E_{\Delta H_\mu W_p c.}\,. \tag{28}$$

Replacing the approximate equality by the exact one yields

$$\Delta H_{\mu_{s.l.c.W_p}} = C_6 e^{\frac{-\Delta E_{\Delta H_\mu W_p c.}}{W_p}}\,, \tag{29}$$

where $C_6 = \Delta H_{\mu_{s.l.c.W_{p\max}}}$; $\Delta H_{\mu_{s.l.c.W_{p\max}}}$ is the greatest microhardness of the strengthened layer. Then,

$$\Delta H_{\mu_{s.l.c.W_p}} = \Delta H_{\mu_{s.l.c.W_{p\max}}} e^{\frac{-\Delta E_{\Delta H_\mu W_p c.}}{W_p}}\,. \tag{30}$$

Dependence (30) can be taken into account as an equation of the microhardness of the strengthened layer depending on the discharge energy. If, in Eq. (30),

$$\Delta E_{\Delta H_\mu W_p c.} = W_p\,, \tag{31}$$

$$\Delta H_{\mu_{s.l.c.W_p}} \Big/ \Delta H_{\mu_{s.l.c.W_{p\max}}} = e^{-1}\,. \tag{32}$$

Thus, the activation energy $\Delta E_{\Delta H_\mu W_p c.}$ is a physical value that is equal to the discharge energy W_p, at which the microhardness of the strengthened layer is e times less than its maximum value. The value $\Delta E_{\Delta H_\mu W_p c.}$ can be determined by the constant of the equation of the microhardness of the strengthened layer depending on the discharge energy. The other constant of this equation, $\Delta H_{\mu_{s.l.c.W_{p\max}}}$, is the greatest microhardness of the strengthened layer.

The greatest microhardness of the strengthened layer $\Delta H_{\mu_{s.l.c.W_{p\max}}}$, namely, the constant of the equation of the microhardness of the strengthened layer, can be determined by the value of the segment cut off on the ordinate axis by the point of the intersection of the extended straight line of the graph of the dependence of the logarithm of the microhardness of the strengthened layer ($\ln \Delta H_{\mu_{s.l.c.W_{p\max}}}$) of steel 20 and steel 40 on the value of the reciprocal discharge energy. The other constant of the equation of the thickness of the strengthened layer, the activation energy, is determined as $\Delta E_{\Delta H_\mu W_p c.} = \mathrm{tg}\alpha$ with being the angle of inclination of the straight lines of the dependences of $\ln \Delta H_{\mu_{s.l.c.Wp}}$ on $1/W_p$.

Further, we consider the effect of the labour-intensiveness, τ, on the increase in microhardness of the strengthened layer, $\Delta H_{\mu_{s.l.c.}} = f(\tau)$.

As follows from the correlation dependence of the increase in the microhardness of the strengthened layer on the value of the reciprocal labour-intensiveness, the logarithm of the increase in the microhardness of the strengthened layer

$$\ln \Delta H_{\mu_{s.l.c.\tau}} \propto -\tau^{-1}. \tag{33}$$

Passing from the approximate to the exact equality, we obtain:

$$\Delta H_{\mu_{s.l.c.\tau}} = C_7 e^{\frac{-1}{\tau}}, \tag{34}$$

where $C_7 = \Delta H_{\mu_{s.l.c.}\tau_{\max}}$ ($\Delta H_{\mu_{s.l.c.}\tau_{\max}}$ is the greatest increase in microhardness of the strengthened layer). Then,

$$\Delta H_{\mu_{s.l.c.\tau}} = \Delta H_{\mu_{s.l.c.\tau_{\max}}} e^{\frac{-1}{\tau}}. \tag{35}$$

Dependence (30) can be considered as an equation of the increase in the microhardness of the strengthened layer depending on the labour-intensiveness at the ESC process.

The greatest increase in the microhardness of the strengthened layer $\Delta H_{\mu_{s.l.c.}\tau_{\max}}$, namely, the constant of the equation of the increase in the microhardness of the strengthened layer depending on the labour-intensiveness, can be determined using the value of the segment cut off on the ordinate axis by the point of the intersection of the extended straight line of the graph of the dependence of the logarithm of the increase in the microhardness of the strengthened layer $\ln\Delta H_{\mu_{s.l.c.\tau}}$ of steel 20 and steel 40 on the value of the reciprocal labour-intensiveness $1/\tau$.

Considering that the total increase in the microhardness of the strengthened layer depends on the discharge energy and labour-intensiveness, $\Delta H_{\mu_{s.l.c.}} = f(W_p, \tau)$, after the conducted studies, it is quite possible to conclude that

$$\Delta H_{\mu_{s.l.c.}} = \Delta H_{\mu_{s.l.c.W_{p\max}}} e^{\frac{-E_{\Delta H_\mu W_p c.}}{W_p}} + \Delta H_{\mu_{s.l.c.\tau_{\max}}} e^{\frac{-1}{\tau}}. \tag{36}$$

Table 17. **The constants of equations of the thickness of the strengthened layer and its microhardness at ESC processing steels 20 and 40 with the use of the ESA method [94]. Here, the numerator is the value of the constants for steel 20; the denominator is for steel 40**

ESA modes	$\Delta h_{s.l.c.W_{p\max}}$, μm	$\Delta E_{\Delta h W_p c.}$ as tgα	$\Delta h_{s.l.c.\tau_{\max}}$, μm	$\Delta H_{\mu_{s.l.c.W_{p\max}}}$, MPa	$E_{\Delta H_\mu W_p c.}$ as tgα	$\Delta H_{\mu_{s.l.c.\tau_{\max}}}$, MPa
Existing modes	236.8/240.2	0.711/0.713	—	12419/12402	1.225/1.225	—
Option 1	248.9/256.5	0.717/0.721	35.9/44.6	12495/12517	1.226/1.227	287.1/224.3
Option 2	255.5/268.7	0.720/0.727	43.0/46.9	12571/12570	1.227/1.227	431.5/253.6
Option 3	259.1/273.7	0.722/0.730	41.5/40.9	12597/12588	1.228/1.228	187.4/224.3

Expression (36) can be considered as an equation of the increase in the microhardness of the strengthened layer depending on the ESA parameters.

Table 17 represents the summarized data of the constants of the equations of the thickness of the strengthened layer and its microhardness at the ESC processes for steel 20 and steel 40.

4. Conclusions

(i) When NESC and ESC processing the C22 steel and the C40 steel, previously processed by the ESA method with aluminium, there increases the thickness, microhardness and continuity of the 'white' layer, while the roughness changes slightly.

(ii) Precisely processing by the ESA method with aluminium at $W_p < 0.13$ J does not result in noticeable changes in the quality parameters of the surface layers formed at all processing types, and, at $W_p > 3.40$ J, it is accompanied by a sharp increase in the roughness of the surface layer. For practical application, the recommended parameters are in the range of $W_p = 0.13–3.4$ J for the NESC process, and those ones are in the range of $W_p = 0.13–4.6$ J for the ESC process.

(iii) The analysis of the phase composition has shown that the presence of an aluminium sublayer results in the formation of the aluminium-containing phases, which cause a significant increase in the hardness and thickness of the surface layers.

(iv) The proposed NESC and ESC technologies can be used to strengthen the surface layers of the critical parts and their elements for compressor and pump equipment, namely: the external and internal surfaces of the protective sleeves for the floating seals, the end surfaces of their rings and the connecting parts for their housings and covers; the bearing necks for the rotor shafts of the centrifugal machines; the piston rods, *etc*.

(v) In case of the NESC processing,

compared to nitriding, the thickness of the strengthened surface layer and its microhardness increase;

with increasing the discharge energy, there increases the thickness of the 'white' layer and the diffusion zone, as well as the microhardness, roughness and surface continuity;

with decreasing the ESA productivity, the thickness of the strengthened surface layer and its microhardness increase, as well as the continuity of the coating improves;

when replacing the steel 20 substrate with steel 40, the thickness of the strengthened surface layer and its microhardness increase slightly.

(vi) In case of the ESC processing,

a surface layer is formed, which, as compared to the layer after NESC processing, has a greater thickness of the strengthened zone and a higher microhardness value;

with an increase in the discharge energy, the thickness of the strengthened layer and its microhardness, as well as the roughness and the continuity of the coating, increase;

with a decrease in the ESA process productivity and, accordingly, an increase in the labour-intensiveness thereof, the thicknesses of the 'white' layer and the diffusion (transition) zone increase, as well as the microhardness and the continuity of the coating;

when replacing steel 20 with steel 40, the thickness of the 'white' layer, the diffusion (transition) zone and the microhardness of the surface increase slightly.

(vii) Due to the research, there have been developed the mathematical models of the dependences of the surface quality values at NESC and ESC processing by the ESA method with the use of the STSMs (the equation of the increase in the thickness of the strengthened layer and the equation of the increase in the microhardness of the surface) on the energy and technological parameters of the ESA equipment: the discharge energy (W_p) and the labour-intensiveness (τ), respectively. This event allows determining the main technological parameters of the formed layer, *i.e.*, the thickness of the strengthened layer and its microhardness, and, thus, improving the technology of manufacturing and repairing the critical parts of the dynamic equipment depending on the requirements imposed on them.

(viii) There has been developed a procedure for determining the constants for the equations of the increase at the NESC and ESC processes by the ESA method: the thickness of the strengthened layer (the greatest increase in the thickness of the strengthened layer depending on the discharge energy and the activation energy), the greatest increase in the thickness of the strengthened layer depending on the labour-intensiveness of the ESA process, as well as the equation for the increase in the surface microhardness (the greatest increase in the microhardness of the strengthened layer depending on the discharge energy and the activation energy), the greatest increase in the microhardness of the strengthened layer depending on the labour-intensiveness of the ESA process.

Acknowledgements. The authors acknowledge that some of the results were obtained within the research project 'Development of environmentally safe technologies for surface modification of power plant equipment parts using combined methods based on electrospark alloying' (state reg. No. 0124U000539) carried out at Sumy State University and funded by the Ministry of Education and Science of Ukraine. This work was also supported by the National Research Foundation of Ukraine under project No. 2025.07/0115.

Authors' Contributions. V.B.T. reviewed and analysed the research results presented in Pt. 1 [1] of this work, as well as the existing literature, and defined the aim and objectives of the study. He substantiated the necessity of preliminary aluminium treatment of components to improve the quality parameters of modified steel surfaces using nitrogen–carbon constituents of the specialised saturating technological medium, specifically, increasing the coating thickness, microhardness, and continuity with only a slight increase in surface roughness. O.P.H. developed a mathematical model for predicting the quality parameters of surface layers of steel components during electrospark carburizing using the electrospark alloying method. She supervised the research outcomes and prepared the manuscript with the participation of all authors; she formulated the general conclusions. N.V.T. developed a mathematical model for predicting the quality parameters of surface layers of steel components during electrospark carburizing by the electrospark alloying method. She also formatted the references in accordance with established requirements. Ie.V.K. identified and analysed the dependences of surface quality parameters of components on the energy and technological parameters of electrospark alloying using saturating technological medium during electrospark nitrocarburizing. M.A.M. and S.G.B. prepared the tables and figures in accordance with established requirements. All authors approved the final version of the manuscript.

REFERENCES

1. V.B. Tarelnyk, O.P. Haponova, N.V. Tarelnyk, Ie.V. Konoplianchenko, M.A. Mikulina, and V.V. Postolatii, Improving the quality parameters of steel surfaces by combined electrospark carburizing technologies. Pt. 1. Properties of metal surfaces, *Prog. Phys. Met.*, **27**, No. 2: 304 (2026); https://doi.org/10.15407/ufm.27.02.304
2. O. Gaponova, C. Kundera, G. Kirik, V. Tarelnyk, V. Martsynkovskyy, Ie. Konoplianchenko, M. Dovzhyk, A. Belous, and O. Vasilenko, *Advances in Thin Films, Nanostructured Materials, and Coatings. NAP 2018. Lecture Notes in Mechanical Engineering* (Singapore: Springer: 2019), p. 249; https://doi.org/10.1007/978-981-13-6133-3_25
3. V. Savulyak, O. Shilina, V. Shenfeld, and A. Osadchuk, *Probl. Tribology*, **27**, No. 1/103: 58 (2022); https://doi.org/10.31891/2079-1372-2022-103-1-58-64
4. V.V. Knysh, S.O. Solovei, B.N. Mordyuk, V.V. Savitsky, O.L. Mikhodui, D.A. Lesyk, and S.I. Motrunich, *Int. J. Fatigue*, **181**: 108147 (2024); https://doi.org/10.1016/j.ijfatigue.2024.108147
5. V.V. Knysh, S.O. Solovei, L.M. Lobanov, O.L. Mikhodui, P.Yu. Volosevich, D.A. Lesyk, A.P. Burmak, and B.N. Mordyuk, *J. Mater. Eng. Perform.*, **33**: 7537 (2024); https://doi.org/10.1007/s11665-024-09355-0
6. L. Nyrkova, V. Knysh, S. Solovei, and S. Osadchuk, *Mater. Protection*, **65**: 680 (2024); https://doi.org/10.62638/ZasMat1052
7. F.A.P. Fernandes, S.C. Heck, R.G. Pereira, A. Lombardi-Neto, G.E. Totten, and L.C. Casteletti, *J. Achiev. Mater. Manuf. Eng.*, **40**, No. 2: 175 (2010).
8. S.H. Yeh, L.H. Chiu, and H. Chang, *Engineering*, **9**, No. 3: 942 (2011); https://doi.org/10.4236/eng.2011.39116
9. S. Ben Slima, *Mater. Sci. Applic.*, **9**, No. 3: 640 (2012); https://doi.org/10.4236/msa.2012.39093

10. O.P. Umanskyi, M.S. Storozhenko, V.B. Tarelnyk, N.V. Tarelnyk, and T.V. Kurinna, *Powder Metall. Met. Ceram.*, **59**: 57 (2020); https://doi.org/10.1007/s11106-020-00138-5
11. B.O. Trembach, M.G. Sukov, V.A. Vynar, I.O. Trembach, V.V. Subbotina, O.Yu. Rebrov, O.M. Rebrova, and V.I. Zakiev, Effect of incomplete replacement of Cr for Cu in the deposited alloy of Fe–C–Cr–B–Ti alloying system with a medium boron content (0.5% wt.) on its corrosion resistance, *Metallofiz. Noveishie Tekhnol.*, **44**, No. 4: 493 (2022); https://doi.org/10.15407/mfint.44.04.0493
12. L. Ropyak, I. Schuliar, and O. Bohachenko, *East.-Eur. J. Enterp. Technol.*, **1**, No. 5: 53 (2016) (in Ukrainian); https://doi.org/10.15587/1729-4061.2016.59850
13. I. Ivasenko, V. Posuvailo, H. Veselivska, and V. Vynar, *Int. Sci. Tech. Conf. Computer Sciences and Information Technologies*, **2**: 9321900 (2020); https://doi.org/10.1109/CSIT49958.2020.9321900
14. M. Bembenek, M. Makoviichuk, I. Shatskyi, L. Ropyak, I. Pritula, L. Gryn, and V. Belyakovskyi, *Sensors*, **22**, No. 21: 8105 (2022); https://doi.org/10.3390/s22218105
15. M.M. Student, V.M. Dovhunyk, V.M. Posuvailo, I.V. Koval'chuk, and V.M. Hvozdets'kyi, *Mater. Sci.*, **53**, No. 3: 359 (2017); https://doi.org/10.1007/s11003-017-0083-x
16. I. Pazukha, Y. Shkurdoda, K. Tyschenko, A. Lohvynov, O. Pylypenko, M. Lisnichuk, D. Kondrakhova, V. Latyshev, S. Vorobiov, and V. Komanicky, *Vacuum*, **230**: 113650 (2024); https://doi.org/10.1016/j.vacuum.2024.113650
17. S.A. Kniaziev, H.O. Kniazieva, V.V. Subbotina, O.O. Volkov, and V.A. Riaboshtan, *Phys. Chem. Solid State*, **26**, No. 2: 436 (2025); https://doi.org/10.15330/pcss.26.2.436-441
18. E. Wojtiuk, M. Maździarz, T. Stasiak, M. Brykała, M. Chmielewski, M. Włoczewski, A. Kosińska, K. Zielińska, O. Haponova, J. Jasiński, and T. Mościcki, *J. Alloys Compd.*, **1049**: 185222 (2025); https://doi.org/10.1016/j.jallcom.2025.185222
19. O. Poliarus, O. Umanskyi, V. Konoval, M. Pomorska, M. Szczerba, A. Korniewa-Surmacz, Ł. Maj, and J. Morgiel, *J. Alloys Compd.*, **1037**: 182299 (2025); https://doi.org/10.1016/j.jallcom.2025.182299
20. S. Pylypaka, M. Klendii, T. Kremets, and O. Klendii, *Eng. J.*, **22**, No. 3: 83 (2018); https://doi.org/10.4186/ej.2018.22.3.83
21. S.F. Pylypaka, M.B. Klendii, and O.M. Klendii, *Acta Polytech.*, **58**, No. 3: 201 (2018); https://doi.org/10.14311/AP.2018.58.0201
22. V. Bulgakov, S. Pilipaka, V. Adamchuk, and J. Olt, *Agronomy Res.*, **12**, No. 3: 937 (2014).
23. T. Volina, S. Pylypaka, A. Rebrii, O. Pavlenko, and Y. Kremets, *Advanced Manufacturing Processes II* (Eds. V. Tonkonogyi, V. Ivanov, J. Trojanowska, G. Oborskyi, A. Grabchenko, I. Pavlenko, M. Edl, I. Kuric, and P. Dasic) (Cham: Springer: 2021), p. 237; https://doi.org/10.1007/978-3-030-68014-5_24
24. S. Pylypaka, T. Volina, A. Nesvidomin, I. Zakharova, and A. Rebrii, *Advances in Design, Simulation and Manufacturing IV* (Eds. V. Ivanov, I. Pavlenko, O. Liaposhchenko, J. Machado, and M. Edl) (Cham: Springer: 2021), p. 156; https://doi.org/10.1007/978-3-030-77823-1_16

25. V.A. Tatarenko, T.M. Radchenko, A.Yu. Naumuk, and B.M. Mordyuk, *Prog. Phys. Met.*, **26**, No. 1: 3 (2025);
https://doi.org/10.15407/ufm.26.01.003
26. V.A. Tatarenko, T.M. Radchenko, A.Yu. Naumuk, and B.M. Mordyuk, *Prog. Phys. Met.*, **25**, No. 1: 3 (2024);
https://doi.org/10.15407/ufm.25.01.003
27. D.S. Leonov, T.M. Radchenko, V.A. Tatarenko, and Yu.A. Kunitsky, *Defect Diffus. Forum*, **273–276**: 520 (2008);
https://doi.org/10.4028/www.scientific.net/DDF.273-276.520
28. D.S. Leonov, T.M. Radchenko, V.A. Tatarenko, and Yu.A. Kunitsky, *Metallofiz. Noveishie Tekhnol.*, **29**, No. 12: 1587 (2007) (in Ukrainian).
29. T.M. Radchenko, V.A. Tatarenko, H. Zapolsky, and D. Blavette, *J. Alloys Compd.*, **452**, No. 1: 122 (2008);
https://doi.org/10.1016/j.jallcom.2006.12.149
30. T.M. Radchenko, V.A. Tatarenko, and H. Zapolsky, *Solid State Phenomena*, **138**: 283–302 (2008);
https://doi.org/10.4028/www.scientific.net/SSP.138.283
31. A.D. Pogrebnjak, A.A. Bagdasaryan, P. Horodek, V. Tarelnyk, V.V. Buranich, H. Amekura, N. Okubo, N. Ishikawa, and V.M. Beresnev, *Mater. Lett.*, **303**: 130548 (2021);
https://doi.org/10.1016/j.matlet.2021.130548
32. V. Martsinkovsky, V. Yurko, V. Tarelnik, and Yu. Filonenko, *Procedia Eng.*, **39**: 157 (2012);
https://doi.org/10.1016/j.proeng.2012.07.019
33. V.B. Tarelnyk, O.P. Gaponova, E.V. Konoplyantschenko, N.S. Yevtushenko, and V.A. Gerasimenko, The analysis of a structural state of surface layer after electroerosive alloying. II. Features of formation of electroerosive coatings on special steels and alloys by hard wear-resistant and soft antifriction materials, *Metallofiz. Noveishie Tekhnol.*, **40**, No. 6: 795 (2018);
https://doi.org/10.15407/mfint.40.06.0795
34. V. Martsinkovsky, V. Yurko, V. Tarelnik, and Yu. Filonenko, *Procedia Eng.*, **39**: 148 (2012);
https://doi.org/10.1016/j.proeng.2012.07.019
35. V. Tarelnyk, I. Konoplianchenko, N. Tarelnyk, and A. Kozachenko, *Mater. Sci. Forum*, **968**: 131 (2019);
https://doi.org/10.4028/www.scientific.net/MSF.968.131
36. O.M. Myslyvchenko, O.P. Gaponova, V.B. Tarelnyk, and M.O. Krapivka, *Powder Metall. Met. Ceram.*, **59**: 201 (2020);
https://doi.org/10.1007/s11106-020-00152-7
37. D.B. Hlushkova, V.A. Bagrov, S.V. Demchenko, V.M. Volchuk, O.V. Kalinin, and N.E. Kalinina, *Probl. Atomic Sci. Technol.*, **140**, No. 4: 125 (2022).
38. B.A. Liashenko, Ye.K. Solovykh, V.H. Kaplun, N.V. Lypynska, and P.V. Kaplun, *Technol. Systems*, **46**, No. 2: 55 (2009) (in Ukrainian).
39. V. Tarelnyk, I. Konoplianchenko, V. Martsynkovskyy, A. Zhukov, and P. Kurp, *Advances in Design, Simulation and Manufacturing. DSMIE 2019. Lecture Notes in Mechanical Engineering* (Eds. V. Ivanov, Y. Rong, J. Trojanowska, J. Venus, O. Liaposhchenko, J. Zajac, I. Pavlenko, M. Edl, and D. Perakovic) (Cham: Springer: 2019), p. 382;
https://doi.org/10.1007/978-3-319-93587-4_40
40. Ye.B. Soroka, V.S. Antoniuk, and Ye.K. Solovykh, *Surface Engineering and Product Renovation: Proc. 8th Int. Scientific and Technical Conference (May 27–29, 2008, Yalta)* (Kyiv: 2008), p. 223 (in Ukrainian).

41. E.K. Solovykh, B.A. Lyashenko, A.V. Rutkovsky, E.B. Soroka, and V.S. Antonyuk, *Technol. Systems*, **38**, No. 2: 22 (2007) (in Ukrainian).
42. V.I. Kuzmin, A.A. Mikhal'chenko, O.B. Kovalev, E.V. Kartaev, and N.A. Rudenskaya, *J. Thermal Spray Technol.*, **21**, No. 1: 159 (2012).
43. A.D. Pogrebnjak, V.I. Ivashchenko, P.L Skrynskyy, O.V. Bondar, P. Konarski, K. Zaleski, S. Jurga, and E. Coy, *Composites Part B: Eng.*, **142**: 85 (2018); https://doi.org/10.1016/j.compositesb.2018.01.004
44. O. Maksakova, S. Simoẽs, A. Pogrebnjak, O. Bondar, Y. Kravchenko, V. Beresnev, and N. Erdybaeva, *Mater. Characteriz.*, **140**: 189 (2018).
45. O.D. Pogrebnjak, K.O. Dyadyura, and O.P. Gaponova, Features of thermodynamic processes on contact surfaces of multicomponent nanocomposite coatings with hierarchical and adaptive behaviour, *Metallofiz. Noveishie Tekhnol.*, **37**, No. 7: 899 (2015); https://doi.org/10.15407/mfint.37.07.0899
46. G. Morand, P. Chevallier, L. Bonilla-Gameros, S. Turgeon, M. Cloutier, M. Da Silva Pires, A. Sarkissian, M. Tatoulian, L. Houssiau, and D. Mantovani, *Surf. Interface Analysis*, **53**, No. 7: 658 (2021); https://doi.org/10.1002/sia.6953
47. G. Maistro, S. Kante, L. Nyborg, and Y. Cao, *Surf. Interfaces*, **24**: 101093 (2021); https://doi.org/10.1016/j.surfin.2021.101093
48. V.G. Smelov, A.V. Sotov, and S.A. Kosirev, *ARPN J. Eng. Appl. Sci.*, **9**, No. 10: 1854 (2014).
49. B. Antoszewski and V. Tarelnik, *Applied Mech. Mater.*, **630**: 301 (2014); https://doi.org/10.4028/www.scientific.net/AMM.630.301
50. B. Antoszewski, S. Tofil, M. Scendo, and W. Tarelnik, *IOP Conf. Ser.: Mater. Sci. Eng.*, **233**: 012036 (2017); https://doi.org/10.1088/1757-899X/233/1/012036
51. V. Tarelnyk, I. Konoplianchenko, O. Gaponova, N. Tarelnyk, V. Martsynkovskyy, B. Sarzhanov, O. Sarzhanov, and B. Antoszewski, *Powder Metall. Met. Ceram.*, **58**: 703 (2020); https://doi.org/10.1007/s11106-020-00127-8
52. H. Aghajani, E. Hadavand, N.S. Peighambardoust, and S. Khamenehasl, *Surf. Interfaces*, **18**, No. 4: 100392 (2020); https://doi.org/10.1016/j.surfin.2019.100392
53. N.E. Kalinina, D.B. Hlushkova, O.D. Hrinchenko, V.T. Kalinin, A.I. Voronkov, L.L. Kostina, I.N. Nikitchenko, T.V. Nosova, and A.A. Reznikov, *Probl. Atomic Sci. Technol.*, **120**, No. 2: 151 (2019).
54. O. Melnyk, O. Onishchenko, S. Kurdiuk, M. Bulgakov, O. Fomin, V. Píštěk, and P. Kučera, *J. Mar. Sci. Eng.*, **13**, No. 9: 1624 (2025); https://doi.org/10.3390/jmse13091624.
55. V.B. Tarelnyk, O.P. Gaponova, V.B. Loboda, E.V. Konoplyanchenko, V.S. Martsinkovskii, Yu.I. Semirnenko, N.V. Tarelnyk, M.A. Mikulina, and B.A. Sarzhanov, *Eng. Appl. Electrochem.*, **57**: 173 (2021); https://doi.org/10.3103/S1068375521020113
56. V.B. Tarelnyk, A.V. Paustovskii, Y.G. Tkachenko, E.V. Konoplianchenko, V.S. Martsynkovskyi, and B. Antoszewski, *Powder Metall. Met. Ceram.*, **55**: 585 (2017); https://doi.org/10.1007/s11106-017-9843-2
57. V. Antonyuk and L. Lopata, *Probl. Tribology*, **30**, No. 2/116: 77 (2025); https://doi.org/10.31891/2079-1372-2025-116-2-77-83
58. V. Martsynkovskyy, V. Tarelnyk, I. Konoplianchenko, O. Gaponova, and M. Dumanchuk, *Advances in Design, Simulation and Manufacturing II. DSMIE 2019.*

Lecture Notes in Mechanical Engineering (Eds. V. Ivanov, Y. Rong, J. Trojanowska, J. Venus, O. Liaposhchenko, J. Zajac, I. Pavlenko, M. Edl, and D. Perakovic (Cham: Springer: 2020);
https://doi.org/10.1007/978-3-030-22365-6_22
59. V.B. Tarel'nik, A.V. Paustovskii, Y.G. Tkachenko, V.S. Martsinkovskii, E.V. Konoplyanchenko, and K. Antoshevskii, *Surface Engineering and Applied Electrochemistry*, **53**, No. 3: 285 (2017);
https://doi.org/10.3103/S1068375517030140
60. V.S. Martsynkovskyi, V.B. Tarelnyk, O.H. Pavlov, and A.O. Ishchenko, *Sposib Vidnovlennya Znoshenykh Poverkhon Metalevykh Detalei (Varianty)* [Method for Restoring Worn Surfaces of Metal Parts (Variants)]: *Patent 104664 UA*, IPC B23H 5/00 (Bul. 4) (2014) (in Ukrainian).
61. V.S. Martsynkovskyi, *Sposib Obrobky Vkladyshiv Pidshypnykiv Kovzannya* [Method of Processing Plain Bearing Liners]: *Patent 77906 UA*, IPC B23H1/00, 3/00, 5/00 (Bul. 1) (2007) (in Ukrainian).
62. V.S. Martsynkovskyi, V.B. Tarelnyk, O.H. Pavlov, and A.O. Ishchenko, *Sposib Vidnovlennya Znoshenykh Poverkhon Metalevykh Detalei (Varianty)* [Method for Restoring Worn Surfaces of Metal Parts (Variants)]: *Patent 104664 UA*, IPC B23H5/00, B23H9/00 (Bul. 4) (2012) (in Ukrainian).
63. V.B. Tarel'nyk, O.P. Gaponova, Ye.V. Konoplyanchenko, and M.Ya. Dovzhyk, Investigation of Regularities of the Processes of Formation of Surface Layers with Electroerosive Alloying. Part I, *Metallofiz. Noveishie Tekhnol.*, **38**, No. 12: 1611 (2016);
https://doi.org/10.15407/mfint.38.12.1611
64. V.B. Tarelnyk, O.P. Gaponova, I.V. Konoplianchenko, and M.Ya. Dovzhyk, Investigation of Regularities of the Processes of Formation of Surface Layers with Electroerosive Alloying. Part II, *Metallofiz. Noveishie Tekhnol.*, **39**, No. 3: 363 (2017);
https://doi.org/10.15407/mfint.39.03.0363
65. V.B. Tarelnyk, O.P. Gaponova, I.V. Konoplianchenko, V.A. Herasymenko, and N.S. Evtushenko, The Analysis of a Structural State of Surface Layer after Electroerosive Alloying. I. Features of Formation of Electroerosive Coatings on Steel 45, *Metallofiz. Noveishie Tekhnol.*, **40**, No. 2: 235 (2018);
https://doi.org/10.15407/mfint.40.02.0235
66. V. Tarelnyk, V. Martsynkovskyy, O. Gaponova, N. Tarelnyk, and S. Gorovoy, *IOP Conf. Ser. Mater. Sci. Eng.*, **233**, No. 1: 012049 (2017);
https://doi.org/10.1088/1757-899X/233/1/012049
67. V.B. Tarelnyk, O.P. Gaponova, N.V. Tarelnyk, and O.M. Myslyvchenko, Aluminizing of Metal Surfaces by Electric-Spark Alloying, *Prog. Phys. Met.*, **24**, No. 2: 282 (2023);
https://doi.org/10.15407/ufm.24.02.282
68. G.V. Kirik, O.P. Gaponova, V.B. Tarelnyk, O.M. Myslyvchenko, and B. Antoszewski, *Powder Metal. Met. Ceram.*, **56**: 688 (2018);
https://doi.org/10.1007/s11106-018-9944-6
69. V. Tarelnyk and V. Martsynkovskyy, *Appl. Mech. Mater.*, **630**: 397 (2014);
https://doi.org/10.4028/www.scientific.net/AMM.630.397
70. V. Tarelnyk, V. Martsynkovskyy, O. Gaponova, Ie. Konoplianchenko, A. Belous, V. Gerasimenko and M. Zakharov, *15th Int. Sci. Eng. Conf. Hermetic Sealing, Vibration Reliability and Ecological Safety of Pump and Compressor Machinery, HERVICON + PUMPS*, **233**, No. 1: 012048 (2017);
https://doi.org/10.1088/1757-899X/233/1/012048

71. V.B. Tarelnik, A.V. Paustovskii, Y.G. Tkachenko, V.S. Martsinkovskii, A.V. Belous, E.V. Konoplyanchenko, and O.P. Gaponova, *Surf. Eng. Appl. Electrochem.*, **54**, No. 2: 147 (2018);
https://doi.org/10.3103/S106837551802014X
72. V. Tarelnyk, O. Gaponova, V. Martsynkovskyy, I. Konoplianchenko, V. Melnyk, V. Vlasovets, M. Mikulina, S. Bondarev, O. Vasilenko, S. Hudkov, A. Kutakh, and G. Golovchenko, *Proc. 2021 IEEE 11th Int. Conf. 'Nanomaterials: Applications and Properties' (05–11 Sept. 2021, Odesa, Ukraine)*;
https://doi.org/10.1109/NAP51885.2021.9568563
73. B. Antoszewski, O.P. Gaponova, V.B. Tarelnyk, O.M. Myslyvchenko, P. Kurp, T.I. Zhylenko, and I. Konoplianchenko, *Materials*, **14**: 739 (2021);
https://doi.org/10.3390/ma14040739
74. O.P. Gaponova, V.B. Tarelnyk, B. Antoszewski, O.M. Myslyvchenko, and J. Hoffman, *Materials*, **15**, No.1: 6085 (2022).
https://doi.org/10.3390/ma15176085
75. A.I. Mikhailyuk and A.E. Gitlevich, *Surf. Eng. Appl. Electrochem.*, **46**: 424 (2010).
76. Y. Kayali and S. Talaş, *Prot. Met. Phys. Chem. Surf.*, **57**: 106 (2021).
77. N. Radek, J. Pietraszek, and A. Szczotok, *Proc. 26th Int. Conf. Metallurgy and Materials (24–26 May 2017, Brno, Czech Republic)*, p. 1432.
78. V.B. Tarel'nik, A.V. Paustovskii, Y.G. Tkachenko, V.S. Martsinkovskii, A.V. Belous, E.V. Konoplyanchenko, and O.P. Gaponova, *Surf. Eng. Appl. Electrochem.* (Allerton Press: New York, NY, USA: 2018), vol. **54**, p. 147.
79. V.B. Tarelnyk, O.P. Gaponova, and Ye.V. Konoplianchenko, Electric-Spark Alloying of Metal Surfaces with Graphite, *Prog. Phys. Met.*, **23**, No. 1: 27 (2022);
https://doi.org/10.15407/ufm.23.01.027
80. O.P. Gaponova, V.B. Tarelnyk, V.S. Martsynkovskyy, Ie.V. Konoplianchenko, V.I. Melnyk, V.M. Vlasovets, O.A. Sarzhanov, N.V. Tarelnyk, M.O. Mikulina, A.D. Polyvanyi, G.V. Kirik, and A.B. Batalova, Combined Electrospark Running-in Coatings of Bronze Parts. Part 1. Structure and Mechanical Properties, *Metallofiz. Noveishie Tekhnol.*, **43**, No. 8: 1121 (2021);
https://doi.org/10.15407/mfint.43.08.1121
81. V.B. Tarelnyk, V.S. Martsynkovskyi, O.P. Haponova, O.A. Sarzhanov, Ye.V. Konoplianchenko, O.O. Hapon, A.D. Lazarenko, and M.O. Mikulina, *Sposib Azotuvannya Poverkhon Stalevykh Detalei* [Method of Nitriding Surfaces of Steel Parts]: *Patent 145506 UA*, IPC C23C 8/00, C23C 8/26 (2006.01), C23C 14/06 (Bul. 23) (2020) (in Ukrainian).
82. E. Wolowiec-Korecka, J. Michalski, and B. Kucharskac, *Vacuum*, **155**: 292 (2018);
https://doi.org/10.1016/j.vacuum.2018.06.025
83. F.G. Wilson and T. Gladman, *Int. Mater. Rev.*, **33**: 221 (1988);
https://doi.org/10.1179/imr.1988.33.1.221
84. *Handbook of Metallurgical Process Design* (Eds. G.E. Totten, K. Funatani, and L. Xie) (Boca Raton, FL, USA: CRC Press: 2004).
85. B. Sun, Z. Liu, Y. He, F. Cao, and X. Li, *Corros. Sci.*, **187**: 109505 (2021);
https://doi.org/10.1016/j.corsci.2021.109505
86. V. Tarelnyk, Yu. Konoplyanchenko, O. Gaponova, M. Dumanchuk, and V. Martsynkovsky, *Advances in Design, Simulation and Manufacturing II. DSMIE 2019. Lecture Notes in Mechanical Engineering* (Berlin–Heidelberg: Springer: 2020), p. 216.
87. V.B. Tarelnyk, V.S. Martsynkovskyi, O.P. Haponova, O.A. Sarzhanov, Ye.V. Konoplianchenko, O.O. Hapon, A.D. Lazarenko, and M.O. Mikulina, *Sposib Nitrotsementatsii Poverkhon Stalevykh Detalei* [Method of Nitrocarburizing Surfaces of Steel Parts]: *Patent 146373 UA*, IPC C23C 8/00, C23C 8/22/ (Bul.7) (2021) (in Ukrainian).

88. N.V. Tarelnyk, *Technological Features of Surface Modification of Nuclear Power Plant Pump Parts* (Sumy: Universytetska Knyha: 2024) (in Ukrainian).
89. V.B. Tarelnyk, O.P. Gaponova, G.V. Kirik, Ye.V. Konoplianchenko, N.V. Tarelnyk, and M.O. Mikulina, Cementation of Steel Details by Electrospark Alloying, *Metallofiz. Noveishie Tekhnol.*, **42**, No. 5: 655 (2020); https://doi.org/10.15407/mfint.42.05.0655
90. V.B. Tarelnyk, O.P. Haponova, N.V. Tarelnyk, and I.L. Rogovskii, *Probl. Atomic Sci. Technol.*, No. 2: 131 (2025); https://doi.org/10.46813/2025-156-131
91. G.F. Vander Voort, *Metallography and Microstructures* (Materials Park, OH, USA: ASM International: 2004).
92. N.V. Tarelnyk, D.B. Hlushkova, O.P. Haponova, Ie.V. Konoplianchenko, and V.O. Skrypnikov, *Functional Mater.*, **32**, No. 2: 223 (2025); https://doi.org/10.15407/fm32.02.223
93. N.V. Tarelnyk, Development of Technological Foundations for Surface Modification of Pump Parts for Nuclear Power Plants with the Use of Combined Environmentally Friendly Methods, *Abstract of Thesis for Dr. Tech. Sci.* (Kharkiv: National Technical University 'Kharkiv Polytechnic Institute': 2025), 42 p.
94. N.V. Tarelnyk, Development of Technological Foundations for Surface Modification of Pump Parts for Nuclear Power Plants with the Use of Combined Environmentally Friendly Methods, *Thesis for Dr. Tech. Sci.* (Kharkiv: National Technical University 'Kharkiv Polytechnic Institute': 2025).

Received / Final version
02.04.2026 / 02.08.2026

В.Б. Тарельник[1], О.П. Гапонова[2,3], Є.В. Коноплянченко[1], Н.В. Тарельник[1], С.Г. Бондарев[1], М.О. Мікуліна[1]
[1] Сумський національний аграрний університет, вул. Герасима Кондратьєва, 160, 40021 Суми, Україна
[2] Сумський державний університет, вул. Харківська, 116, 40007 Суми, Україна
[3] Інститут фундаментальних технологічних досліджень, Польська академія наук, 5Б Павіньскєґо, 02-016 Варшава, Польща

ПІДВИЩЕННЯ ПАРАМЕТРІВ ЯКОСТІ СТАЛЕВИХ ПОВЕРХОНЬ КОМБІНОВАНИМИ ТЕХНОЛОГІЯМИ ЕЛЕКТРОІСКРОВОЇ ЦЕМЕНТАЦІЇ.

Ч. 2. Математичні моделі для регулювання властивостей металевих поверхонь

Сучасне машинобудування базується на новітніх досягненнях науки та техніки, що зумовлює необхідність використання надійних і безвідмовних інженерних рішень, які впливають на надійність і довговічність деталей машин, що працюють у важких умовах інтенсивних навантажень, екстремальних температур і корозійних середовищ. Розв'язання цих проблем потребує вдосконалення технологічних основ поверхневого модифікування деталей машин екологічно безпечними методами, що є вкрай актуальним завданням. У роботі доведено, що серед сучасних технологій найбільшої уваги заслуговує метод електроіскрового легування (ЕІЛ), завдяки якому в поверхневих шарах формуються структури з унікальними фізико-механічними та трибологічними властивостями. Метою роботи є розроблення адекватної, фізично обґрунтованої математичної моделі прогнозування параметрів якості поверхневих шарів сталевих деталей під час електроіскрової цементації (ЕЦ) та нітроцементації (НЕЦ) методом електроіскрового легування залежно від енергетичних і технологічних параметрів обладнання ЕІЛ із використанням спеціального технологічного насичувального середовища (СТНС). Наведено результати досліджень впливу попереднього оброблення деталей Алюмінієм на параметри якості модифікованих сталевих поверхонь із використанням СТНС у вигляді нітрогенкарбонових компонентів. Аналіз фазового складу показав, що наявність алюмінієвого підшару спричиняє утворення алюмінієвмісних фаз, що зумовлює значне підвищення твердості та товщини поверхневих шарів. Експериментально визначено залежності параметрів якості поверхонь деталей від енергетичних і технологічних параметрів ЕІЛ під час НЕЦ і ЕЦ. Також розроблено математичні моделі залежности якості поверхонь за умов НЕЦ і ЕЦ (рівняння приросту товщини зміцненого шару та рівняння приросту мікротвердості поверхні) від енергетичних і технологічних параметрів обладнання ЕІЛ, що дає змогу визначати основні технологічні параметри сформованого шару — товщину зміцненого шару та його мікротвердість. Розроблено методику визначення констант рівнянь приросту за умов НЕЦ і ЕЦ: товщини зміцненого шару (з урахуванням максимального приросту залежно від енергії розряду та трудомісткості, а також енергії активації) та мікротвердості (з урахуванням максимального приросту залежно від енергії розряду, трудомісткості й енергії активації). Запропоновані математичні моделі можуть бути використані для зміцнення поверхневих шарів деталів компресорного та насосного обладнання: захисних втулок, торцевих поверхонь кілець, сполучних частин корпусів і кришок, підшипникових шийок валів відцентрових машин тощо.

Ключові слова: електроіскрове легування, цементація, нітроцементація, зміцнений шар, математичне моделювання.